Chapter 2

Photochemistry of Allyl-Tetrazolyl Derivatives in Solution

As refered previously in Chapter one, the photochemistry of a series of allyl-tetrazoles in solution was investigated. Several important mechanistic questions concerning the photodecomposition of these compounds in different solvents were answered, and new synthetic methodologies for the preparation of heterocyclic compounds from allyl-tetrazoles were developed.

The work described in this Chapter is included in the following international scientific journals: *Tetrahedron Letters*, **2005**, *76*, 6757-6760, *Journal of Organic Chemistry,* **2006**, *71*, 3583-3591 and *Organic & Biomolecular Chemistry*, **2008**, *6*, 1046-1055. The contents of these publications are partly reproduced below.

2.1. Introduction

The relevance of tetrazolyl compounds stimulated research in their structure and reactivity. Special attention has been devoted to heteroaromatic ethers derived from tetrazole, with important practical uses as intermediate compounds in the transformation of alcohols.[1-3] Compounds bearing an allylic alcohol function are frequently vital structural units of biologically active systems and have also attracted widespread attention as key intermediates in synthesis.[4-6] It was reported previously that selective hydrogenolysis of the C–OH bond of allyl alcohols can be achieved conveniently by first reacting the alcohol with 5-chloro-1-phenyltetrazole[7] so as to form the heteroaromatic allyl ether **1** (Figure 1), which will then undergo smooth heterogeneously catalyzed transfer hydrogenolysis to form the alkene **3**, corresponding to the allyl group, and phenyltetrazolone **4**.[8] In ethers **1**, which can be regarded as imidates, the heteroaromatic group together with the oxygen atom from the original allyl alcohol acts as an excellent leaving group in catalysed *ipso*-substitutions.

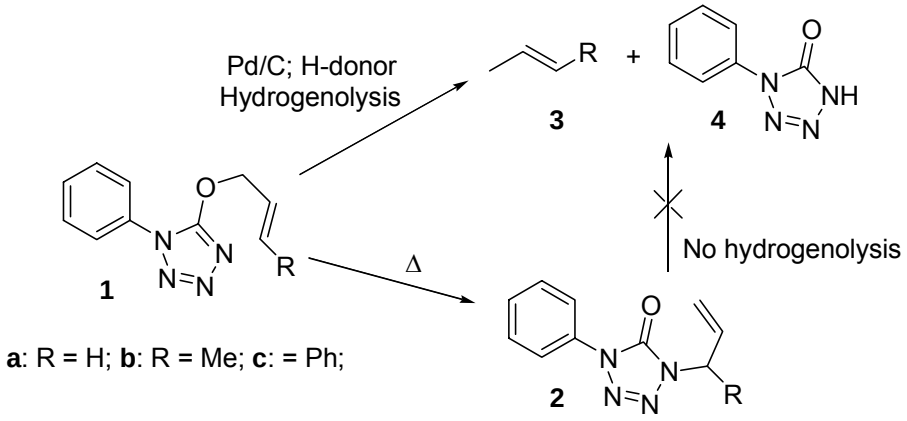

Figure 1. Hydrogenolysis of the C-O bond and competitive thermal isomerization of 5-allyloxy-1-aryl tetrazoles.

Selective heterogeneous catalytic transfer reduction of such allyl ethers is quite remarkable, because it successfully competes with hydrogenation of the double bond and also with the relatively easy [3,3]-sigmatropic rearrangement to give the *N*-allyl isomers **2**. Thermal *O*- to *N*- migration of the allyl group in a series of 5-allyl-tetrazolyl compounds **1**, (Figure 1), proceeds exclusively in a [3,3]-sense through a polar chair-like transition state, to give *N*-allyl-tetrazolones **2** as sole products.[9,10] This behavior is similar to the notionally comparable general Cope rearrangement, which proceeds through an allowed [3,3]-mechanism,[11-16] and is known to be catalysed by transition metals. It was found that thermal isomerization of 5-cinamyloxy-1-phenyl-tetrazole (**1c**) is three times faster in the presence of Pd than in its absence.[8] Therefore, it was specially important that hydrogenolysis of allyl tetrazolyl ethers **1** occurs in less than 10 min, at room temperature. It is also of interest to note that no hydrogenolysis of the C–N bond was observed even upon extended reactions times and increase in temperature.

In view of the widespread interest in tetrazoles and allylic compounds, and encouraged by the rich photochemistry of several tetrazole derivatives, we elected two series of allyl-tetrazolyl derivatives as object of photochemical study: allyl ethers **1a**–**c** and allyl-tetrazolones **2a**–**c**.

In Section 2.2., results on the photolysis (λ = 254 nm) of 4-allyl-tetrazolones **2a**–**c** in methanol, 1-propanol, 1-hexanol, acetonitrile, and cyclohexane are presented and discussed. During this study, the sole primary photochemical process identified was molecular nitrogen elimination, with formation of 3,4-dihydro-6-substituted-pyrimidinones. Following the primary photocleavage, secondary reactions were observed in acetonitrile and cyclohexane, leading to phenylisocyanate, aniline and 1-phenylprop-1-enyl-isocyanate. In alcoholic solutions, the primary products, remained photostable even under extended irradiation, making possible the isolation of 3,4-dihydro-pyrimidinones as stable compounds in very high yields. The observed photostability of pyrimidinones in alcohols is ascribed to the excited state quenching *via* reversible proton transfer, facilitated by the solvent cage stabilization due to formation of hydrogen bonds. The viscosity of alcohols is directly related to the cage effects observed. The photocleavage of 4-allyl-tetrazolones leads probably to a caged triplet radical pair. This hypothesis is confirmed by the solvent viscosity effect on the photolysis quantum yields. Additionally, dissolved molecular oxygen sensitizes the formation of pyrimidinones, as should be expected for a triplet intermediate that can only form the product molecule after T−S conversion, which is accelerated by oxygen.

In Section 2.3., the photochemistry of 5-allyloxy-tetrazoles **1a-c**, in methanol, acetonitrile and cyclohexane, studied by product analysis and laser flash photolysis, is discussed. The exclusive primary photochemical process identified was molecular nitrogen elimination, with formation of 1,3-oxazines. These compounds were isolated in reasonable yields by column chromatography on silica gel and were fully characterized. DFT(B3LYP)/6-31G(d,p) calculations predict that these 1,3-oxazines can adopt two tautomeric forms: (i) with the NH group acting as a bridge connecting the oxazine and phenyl rings and (ii) with the −N= bridge and the proton shifted to the oxazine ring.

Both tautomeric forms are relevant in the photolysis of oxazines in solution. Secondary reactions were observed, leading to the production of phenyl vinyl-hydrazines, enamines, aniline and phenylisocyanate. Transient absorption detected by laser flash photolysis is attributed to the formation of triplet 1,3-biradicals generated from the excited 5-allyloxy-tetrazoles. The 1,3-biradicals are converted into 1,6-biradicals by proton transfer, which after intersystem crossing decay to generate the products. Solvent effects on the photoproduct distribution and rate of decomposition are negligible.

2.2. Mechanistic Investigations into the Photochemistry of 4-Allyl-tetrazolones in Solution: A New Approach to the Synthesis of 3,4-Dihydro-pyrimidinones

The photochemistry (λ = 254 nm) of 4-allyl-tetrazolones **2a**–**c** (Figure 2) in solution, was investigated. Compounds **2** are obtained from the corresponding tetrazolyl ethers **1** (Figure 1), with quantitative conversion, by heating a neat sample.[9] Allyloxytetrazoles **1** are synthesized by the initial reaction of allylic alcohol with sodium hydride, followed by reaction of the resulting alkoxide with 5-chloro-1-phenyltetrazole.

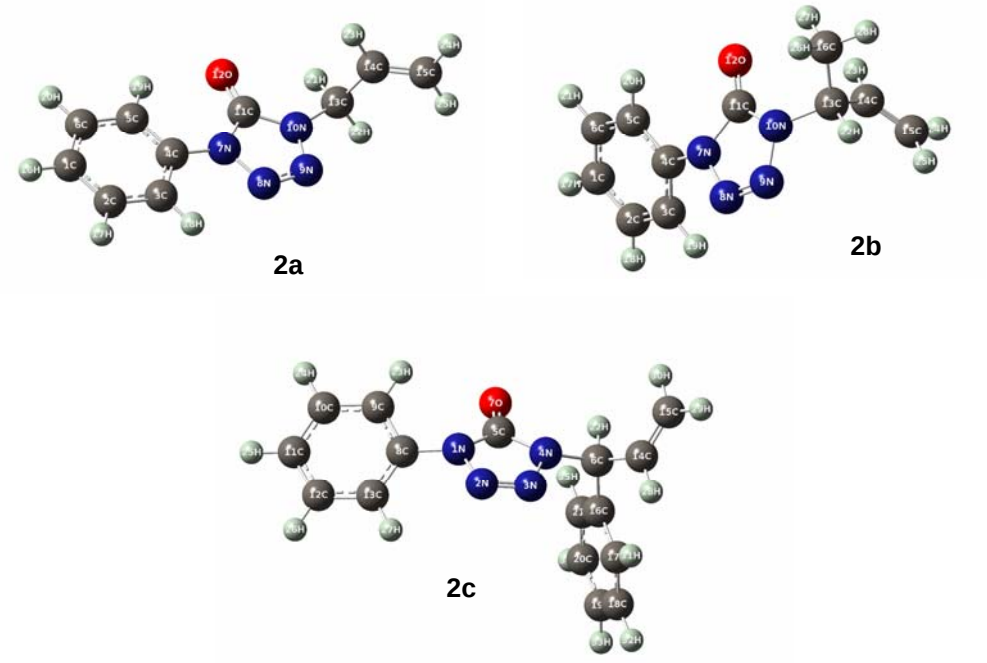

Figure 2. B3LYP/6-31G(d,p) optimized structures of 1-phenyl-4-(prop-2-enyl) tetrazole-5-one (**2a**), 4-(1-methylprop-2-enyl)-tetrazole-5-one (**2b**) and 1-phenyl-4-(1-phenylprop-2-enyl)-tetrazole-5-one (**2c**) with the atom numbering.

To assess the reaction mechanisms involved in the photolysis of 4-allyl-tetrazolones **2a**–**c**, two major aspects were addressed: *(i)* structural elucidation of the photoproducts obtained after UV exposure (λ = 254 nm) of these compounds, in

methanol, 1-propanol, 1-hexanol, acetonitrile and cyclohexane; *(ii)* evaluation of structural effects, the nature of the solvent and the effect of oxygen, on the photoreactivity of compounds **2a**–**c**.

UV spectra of 4-allyl-tetrazolones **2a**–**c** show absorptions around 250 nm. These compounds were irradiated and the progress of the photoreactions was monitored by HPLC. Quantum yields for photocleavage were determined separately. The results obtained are presented and discussed below.

2.2.1. Photolysis of 1-Phenyl-4-(prop-2-enyl) tetrazole-5-one (2a)

Photolysis of 4-allyl-tetrazolone **2a** was initially conducted in methanol. In all experimental conditions tested, *viz*. in air-equilibrated solutions, in solutions saturated with oxygen, or after purging with argon, a single photoproduct, identified as 3,4-dihydro-3-phenylpyrimidin-2(1*H*)-one **5a** (*m/z* = 174), was formed. Complete conversion of **2a** was observed after 65 minutes (Table 1). Extension of the irradiation time to 3 hours did not modify the concentration of the primary photoproduct and no signs of secondary photoproducts were registered.

Isolation of the photoproduct **5a** was carried out simply by solvent evaporation under reduced pressure in mild conditions (92%, isolated yield). The isolated dihydropyrimidinone **5a** is a stable compound, as no degradation was registered during storage. Interestingly, this molecule belongs to a novel structural class of pyrimidinones.[17] 3,4-Dihydro-pyrimidin-2(1*H*)-ones are compounds that have drawn widespread attention, due to their medical applications.[18] For instance, dihydropyrimidinone derivatives have been screened for antihypertension,[19] antibacterial,[20] anti-inflammatory[21] and anticarcinogenic[22] activities or as selective

α_{1a}-andrenergic receptor antagonists.[23] The described synthetic routes to these compounds generally involve multi-step transformations that are essentially based on the Biginelli condensation methodology.[24-26]

The photoreactivity of 4-allyl-tetrazolone **2a** was also assessed in other alcohols. Irradiation of 4-allyl-tetrazolone **2a** in 1-propanol and 1-hexanol, also led to formation of 3,4-dihydro-3-phenylpyrimidin-2(1*H*)-one **5a** as the sole photoproduct. These results point to a single photochemical channel for the photodegradation of **2a**, involving molecular nitrogen extrusion. The time for complete conversion of the substrate increased with the carbon chain length of the alcohol (65 minutes in methanol, 90 in 1-propanol and 190 in 1-hexanol; Table 1).

Table 1. Evolution of substrate concentration [a] in the photolysis [b] of 4-allyl-tetrazolones **2a**–**c**, using different alcohols as solvents.

	Substrate concentration (%)								
	Methanol			1-Propanol			1-Hexanol		
Irradiation time (min)	**2a**	**2b**	**2c**	**2a**	**2b**	**2c**	**2a**	**2b**	**2c**
0.25	93	92	94	95	96	97	98	98	99
0.50	90	89	91	92	94	95	95	95	97
1.0	87	87	89	89	92	92	92	91	95
2.0	83	81	84	85	89	90	88	87	92
4.0	74	75	78	78	84	85	82	84	89
8.0	56	61	62	64	75	78	75	77	85
12	43	49	52	53	65	67	68	67	80
20	32	38	41	40	51	55	56	57	71
40	14	19	23	21	36	40	41	44	61
60	3	6	8	10	17	26	29	32	53
90	-	-	-	3	5	14	23	26	45
120	-	-	-	-	-	5	17	20	37
150	-	-	-	-	-	-	10	13	31
180	-	-	-	-	-	-	3	7	23
210	-	-	-	-	-	-	-	-	15

[a] Relative yields determined by HPLC. [b] λ = 254 nm; initial concentration of the substrates: 1.0×10^{-4} M.

Figure 3 shows the spectra of compounds **2a** and **5a**. Note that the primary product **5a** has some absorbance at the excitation wavelength and thus would reduce the apparent photolysis quantum yields at higher conversions, even in alcoholic solvents.

The product interference becomes a more serious issue in non-alcoholic solvents, as the respective secondary photoproducts have even higher extinction coefficients. The extinction values for compounds **2a**–**c** and **5a**–**c** are given in Table 2. Note that the three starting compounds have similar extinction coefficients and positions of the peak maxima. The values of the extinction coefficients are typical for states of $\pi\pi^*$ nature.

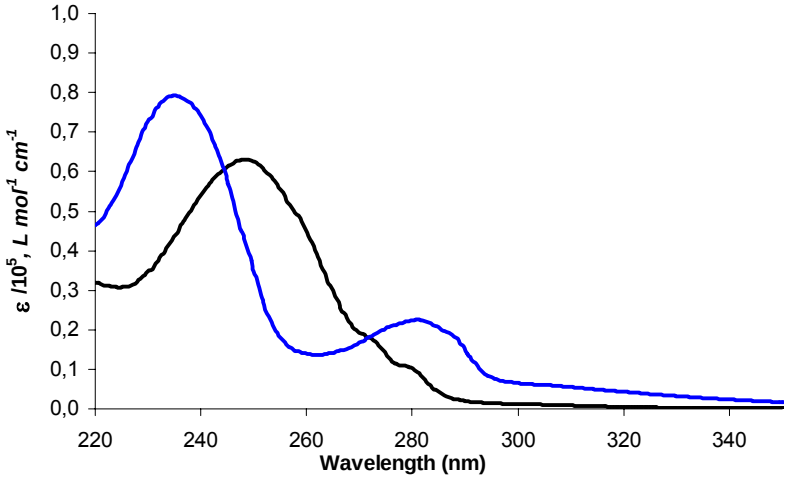

Figure 3. Extinction coefficients (ε) in function of wavelength for tetrazolone **2a** (— *black line*) and pyrimidinone **6a** (— *blue line*) in methanolic solutions.

Table 2. Extinction coefficient values for tetrazolones **2a-c** and pyrimidinones **5a-c** calculated at $\lambda_{max.}$ (results obtained in methanol solution).

Compound	$\lambda_{max.}$ (nm)	$\varepsilon / 10^5$ ($L.mol^{-1}.cm^{-1}$)
2a	249	0.63
2b	249	0.61
2c	250	0.89
5a	235	0.79
5b	233	0.69
5c	231	0.82

The observed photoreactivity for tetrazolone **2a** in acetonitrile and cyclohexane was similar to that in alcohols, but the primary photoproduct **5a** was in turn photolysed. In both solvents, three photoproducts were identified after irradiation: a primary photoproduct (*m/z* = 174) that coincides with the sole photoproduct obtained in alcoholic solutions, and two secondary photoproducts (*m/z* = 93 and 119). Analysis of

the photolyzed samples taken every 2 s allowed for the identification of pyrimidinone **5a** as the primary photoproduct. The other (secondary) photoproducts started to be detectable at irradiation times exceeding 20 s and were identified as phenylisocyanate (**6**, *m/z* = 119) and aniline (**8**, *m/z* = 93) by comparing the HPLC and GC–MS traces with those of standard samples.

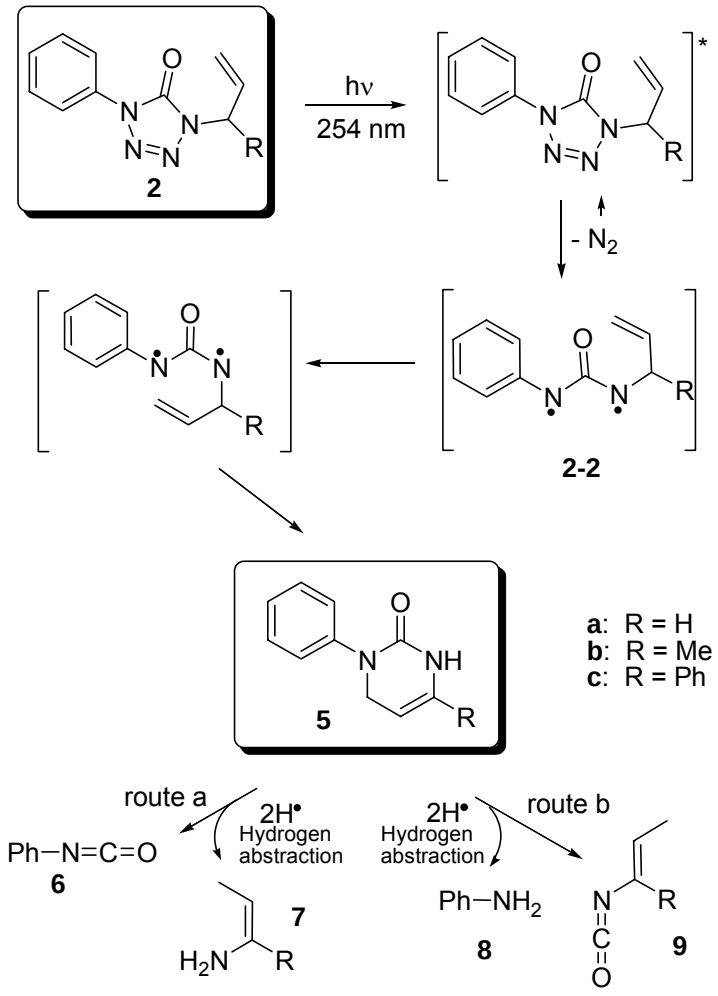

Figure 4. Proposed photodegradation pathways of 4-allyl-tetrazolones **2a-c** in solution.

A single mechanistic route is proposed for the formation of phenylisocyanate, involving the exclusive ring photocleavage of pyrimidinone **5a** (Figure 4, route **a**). This mechanistic approach was confirmed when irradiation experiments using the pure pyrimidinone **5a** (isolated previously from the alcoholic solutions) were done in acetonitrile and cyclohexane. In the course of these experiments, formation of

phenylisocyanate and aniline was detected, confirming that these two secondary photoproducts are a result of pyrimidinone photodegradation.

Two reactive channels could be possible for aniline formation: *(i)* photocleavage of the pyrimidinone ring to give directly the phenyl-nitrene (Ph–N:) intermediate, which would then abstract hydrogen from the solvent to form aniline and *(ii)* initial formation of phenylisocyanate that could undergo subsequent photocleavage to phenyl-nitrene, with elimination of CO, which could also abstract hydrogen to form aniline. However, in view of the experimental observations, we consider that aniline and phenylisocyanate are produced via two independent photochemical channels of degradation of pyrimidinone **5a** (Figure 4, routes **a** and **b**).

Throughout the irradiation experiments, the appearance of these two compounds was detected at the same time, indicating that aniline is formed exclusively by photocleavage of the pyrimidinone ring and does not derive from phenylisocyanate. This hypothesis was confirmed by HPLC analysis of irradiated solutions of phenylisocyanate in acetonitrile and cyclohexane, in conditions similar to those used for allyltetrazolone **2a**. Phenylisocyanate remained photostable upon prolonged irradiation at 254 nm and no aniline formation was ever detected.

The formation of phenylisocyanate and aniline by photocleavage of **5a** will be concomitant with formation of two other possible secondary products, 1-(amino) propene (**7a**) and 1-propenylisocyanate (**9a**), respectively. However, these photoproducts were never detected chromatographically throughout the irradiation experiments, in any of the solvents. This could be explained either by their high volatility, fast photodecomposition into low molecular weight products, and/or very rapid elution in the chromatographic conditions used. The higher photostability of the primary photoproduct **5a** in alcohols against cyclohexane and acetonitrile can be

explained based on solvent stabilization. In alcohols, there might be a strong association between the solvent and the photoproduct involving formation of relatively strong hydrogen bonds. Pyrimidinone **5a** bears several atoms capable of forming hydrogen bonds with solvent molecules (Figure 5). In such conditions, reversible proton transfer could be a fast and efficient mechanism of the excited-state quenching,[27] facilitated by steric limitations resulting from the stable cage enclosing the pyrimidinone molecule and preventing its photodecomposition. Also, the absorbed energy is more efficiently dissipated through the solvated complex, preventing relaxation through pathways leading to photocleavage.

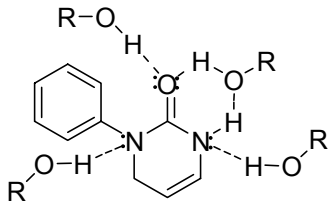

Figure 5. Solvation of pyrimidinone **5a** in alcoholic solutions.

^{1}H-NMR spectra for compound **5a** were obtained in deuterated chloroform, acetonitrile and methanol. In $CDCl_3$ and CD_3OD, all protons connected to carbon atoms show a similar chemical shift. However, in CD_3CN the resonances for the same protons are shifted downfield by 0.25 to 0.35 ppm. The signal due to the resonance of the proton connected to the nitrogen (N–H) appears at 10.2 and 9.1 ppm in $CDCl_3$ and CD_3CN respectively, being absent in CD_3OD.

2.2.2. Photolysis of 4-(1-Methylprop-2-enyl)-tetrazole-5-one (2b) and 1-Phenyl-4-(1-phenylprop-2-enyl)-tetrazole-5-one (2c)

The photochemistry of 4-(1-methylprop-2-enyl)-tetrazole-5-one (**2b**) and 1-phenyl-4-(1-phenylprop-2-enyl)-tetrazole-5-one (**2c**) in solution was investigated using

the methodology described above for tetrazolone **2a**. In methanol (air-equilibrated, oxygen-saturated and argon-purged solutions), photolysis of these two tetrazolones resulted in exclusive formation of the corresponding pyrimidinones **5b** and **5c** (Figure 4), identified as 3,4-dihydro-6-methyl-3-phenylpyrimidin-2(1*H*)-one (*m/z* = 188) and 3,4-dihydro-3,6-diphenylpyrimidin-2(1*H*)-one (*m/z* = 250), respectively. The same behavior was observed when using other alcohols. These pyrimidinones were isolated from the alcoholic solution in excellent yields (97% for **2b** and 90% for **2c**), and no evidence of secondary photoproducts was ever observed when extending the irradiation time. The time required for total photodegradation of 4-allyl-tetrazolones **2a**–**c** in the same alcohol varied for the three compounds (Table 1) increasing from R=H to R=CH_3 and then to R=Ph. As was noted for compound **2a**, the time required for complete conversion also increased with the viscosity of the alcohol.

The present investigation shows that the only photoproduct of **2a**–**c** formed in alcohols, results from N_2 elimination from the tetrazolyl ring system through photo-induced cleavage of the weakest of the N–N formally single bonds ($N_{(7)}$–$N_{(8)}$ and $N_{(9)}$–$N_{(10)}$ for **2a**–**b**; $N_{(1)}$–$N_{(2)}$ and $N_{(3)}$–$N_{(4)}$ for **2c**), (see Figure 2, for atom numbering), leading to the corresponding 3,4-dihydro-6-substituted-3-phenylpyrimidin-6-ones as sole products. Thus, this methodology represents a new synthetic strategy to these compounds, from 5-allylloxytetrazoles **1**, in excellent yields. Chemical diversity may be introduced easily, by changing substituents in the allylic and the tetrazolic systems.[9,17]

In acetonitrile and cyclohexane, the photoreactivity of tetrazolones **2b**,**c** is also similar to that observed for **2a**. In these solvents three photoproducts were identified for compound **2b**: a primary photoproduct (*m/z* = 188) coinciding with the sole photoproduct in methanol and two secondary photoproducts, identified as phenylisocyanate (**6**, *m/z* = 119) and aniline (**8**, *m/z* = 93). The other possible secondary

species formed via photodecomposition of **5b** are 2-amine-2-butene (**7b**) and 1-methylprop-1-enyl-isocyanate (**9b**), Figure 4. However, as for compounds **7a** and **9a**, these predicted photoproducts were never detected in any of the conditions tested during photolysis. Upon photolysis of tetrazolone **2c**, using the same solvents, four photoproducts were identified: the primary photoproduct (*m/z* = 250) that coincides with the sole photoproduct in methanol and three secondary photoproducts identified as phenylisocyanate (**6**, *m/z* = 119), aniline (**8**, *m/z* = 93) and 1-phenylprop-1-enyl-isocyanate (**9c**, *m/z* = 159), Figure 4.

Hence, the results obtained for the photolysis of compounds **2b**–**c** are analogous to those obtained for the photolysis of **2a**, unequivocally demonstrating that their photoreactivity is comparable and that substituent effects on the photoproduct distribution during the photolysis of the 4-allyl-tetrazolones in solution are negligible. However, as a result of an increase in the steric effects (it becomes more difficult for the fragments to separate with growing molecular size) from **2a** to **2c**, the time required for complete photodegradation of the three tetrazolones increases in the same order. As will be shown, similar conclusions follow from analysis of the quantum yield determinations.

Photoinduced loss of nitrogen from compounds **2a**–**c** may involve a cycloelimination leading to a diaziridinone that reacts further to give the observed 3,4-dihydro-6-substituted-3-phenylpyrimidin-2(1*H*)-ones **5a**–**c**, or may occur through a biradical intermediate that subsequently cyclizes to give the same compounds **5a**–**c**. According to the literature, detection of biradical intermediates is not trivial and could not be achieved in this work. In several related investigations such species were detectable only in a limited number of cases.[13] However, based on the experimental results obtained, it is our conviction that a radicalar mechanism operates in this case

(Figure 4). Generally, the transition state in the concerted mechanism (cleavage of two N–N formally single bonds and formation of one new N–N formally single bond and the transformation of N=N double bond into N≡N triple bond) has a higher polarity as compared to that of the initial substrate. Considering the variation in polarity associated with the five solvents used in this work, it appears that the solvent polarity effects are weak or absent during tetrazolone photolysis, contrasting with what could be expected for a concerted process occurring *via* a polar transition state. No production of an urea, via N_2 elimination followed by hydrogen abstraction, has ever been detected. However, this fact is not sufficient to discard the formation of a biradical intermediate in our experiments, because the reactive channel for radical recombination can be much more favorable than the hydrogen abstraction route.

2.2.3. Photolysis Quantum Yields and the Mechanism of Primary Reactions

The quantum yields obtained are rationalized on the basis of the following mechanism of primary reactions, occurring upon photoexcitation of tetrazolones **2a**–**c**:

Scheme 1.

$Substrate + hv \rightarrow Substrate^*$		(*2.1*)
$Substrate^* \rightarrow [R^T \ldots N_2^*]$	ϕ_{pair}	(*2.2*)
$[R^T \ldots N_2^*] \rightarrow Substrate$	k_r	
$[R^T \ldots N_2^*] \rightarrow [R^S \ldots N_2]$	k_{ST}	
$[R^T \ldots N_2^*] + O_2 \rightarrow [R^S \ldots N_2] + O_2^*$	k_q	
$[R^S \ldots N_2] \rightarrow Product + N_2$	*fast*	
$[R^T \ldots N_2^*] \rightarrow R^T + N_2^*$	k_d	
$R^T \rightarrow Product$		

Here, *Substrate* denotes the starting compound **2a**–**c**, *Product* – the reaction product **5a**–**c**, [R^T…N_2*] – the caged radical pair including the triplet biradical **2**–**2** (Figure 4). This reaction scheme is not quite complete, as it should additionally include reencounters between R^T and N_2* that escaped the solvent cage and the reaction between R^T and O_2 in the bulk. However, the complete scheme would be too cumbersome for the analysis and unnecessary for the present purpose, given the lack of time-resolved kinetic data.

Because no fluorescence could be observed from the *Substrates*, we conclude that the reaction (*2.2*) is very fast and, consequently, the respective excited state formed in (*2.1*) and reacting in (*2.2*) is a singlet.

2.2.4. The Effect of Solvent Viscosity

Analysis of the results presented in Table 3 and Figure 6, obtained in argon-purged solutions, shows a direct correlation between the solvent viscosity[28] and the inverse photolysis quantum yield for tetrazolones **2a**–**c**. A good linear correlation is observed for the viscosity variations by one order of magnitude, with the photolysis quantum yields decreasing at higher viscosities. Considering the quantum yields obtained in the five solvents used in this work (Table 3), there is no apparent correlation between the photolysis quantum yields and the solvent dielectric constant. The conjugation of these results with the tetrazolone photoreactivity exhibited in the range of solvents used provides valuable information towards an interpretation of the mechanism that operates through the photolysis.

Table 3. Quantum yields (λ = 254 nm, 25°C) for the photodegradation of 4-allyl-tetrazolones **2a-c**, in the range of solvents used.

		2a	**2b**	**2c**
Solvent (Air-eq.)	Viscosity, η (mPa.s)	Φ_{obs}	Φ_{obs}	Φ_{obs}
Acetonitrile	0.37	0.38	0.35	0.31
Methanol	0.54	0.36	0.34	0.30
Cyclohexane	0.89	0.34	0.31	0.27
1-Propanol	1.95	0.29	0.26	0.23
1-Hexanol	4.58	0.23	0.20	0.17

The observed viscosity dependence clearly points to the importance of the cage effect in the primary reaction mechanism.[29] We believe that the caged radical pair involving species **2**–**2** and N_2 (see Figure 4) is formed as the primary photoproduct, which may either recombine reconstituting the parent molecule **2** (k_r) or escape from the cage (k_d), eventually yielding the photolysis product **5**. The importance of cage effects depends on the relative velocity (and thus the kinetic energy and the mass)[29] of the two fragments, as well as on the solvent viscosity.

Radical cage effects have an enormous impact on chemical reactivity in solution, and in fact they are necessary to explain many fundamental reaction phenomena. These phenomena include rate-viscosity correlations, variations in products and product yields and variations in quantum yields, as a function of medium. Expression (*2.3*) for the product quantum yield results from Scheme 1, in the absence of dissolved oxygen:

$$\phi = \phi_{pair} \frac{k_d + k_{ST}}{k_d + k_{ST} + k_r} \qquad (2.3)$$

Considering $k_d = b/\eta$, we obtain:

$$\frac{1}{\phi} = \frac{1}{\phi_{pair}} \left(1 + \frac{k_r}{\frac{b}{\eta} + k_{ST}} \right) \qquad (2.4)$$

Note that the expression (*2.4*) is linear in η at sufficiently small values of η.

The value of ϕ_{pair} for each one of the three tetrazolones **2a**–**c** is obtained by extrapolating the plot of $1/\phi$ vs. viscosity (Figure 6) to zero viscosity ($\phi_{pair,\ \mathbf{2a}} = 0.39$; $\phi_{pair,\ \mathbf{2b}} = 0.37$; $\phi_{pair,\ \mathbf{2c}} = 0.33$). The reduction of ϕ_{pair} with the size and molecular mass of the radicals should reflect the increasing probability of their re-encounters.[29]

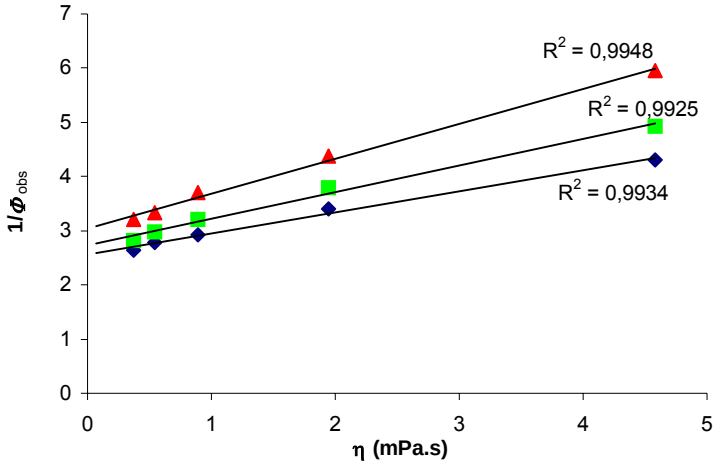

Figure 6. Plot of $1/\phi$ vs. solvent viscosity (η) for the photolysis of 4-allyl-tetrazolones **2a** (◆), **2b** (■) and **2c** (▲) (Argon-purged solutions). Values of viscosity at 25°C: 0.369 (acetonitrile), 0.544 (methanol), 0.894 (cyclohexane), 1.945 (1-propanol), 4.580 (1-hexanol) mPa s.[28]

As expected, the cage effect is increasing with viscosity. Thus, the cage effects can be used to explain the variations of the photolysis quantum yields as a function of medium for 4-allyl-tetrazolones **2a**–**c**.

2.2.5. Effect of Oxygen on the Photoreactivity

It is well known that, in the absence of low lying $^1(\pi,\pi^*)$ or charge transfer states, benzophenones show a high S_1 (n,π^*) to T_1 (n,π^*) intersystem crossing efficiency.[30] Considering the structure of tetrazolones **2a**–**c**, the presence of the carbonyl group in the tetrazole ring is possibly the main structural factor that could make it susceptible to photodegradation proceeding through the lowest triplet states. However, in the particular case of photolysis of compounds **2a**–**c**, we suppose that the

reaction proceeds via a short-lived singlet excited state that quickly leads to a triplet biradical [Scheme 1, reactions (*2.1*) and (*2.2*)].

Contrarily to what should be expected for a triplet-mediated photoprocess, the presence of O_2, an efficient quencher of triplet states, was found to accelerate the photodegradation of tetrazolones in all of the tested solvents (see Table 4, for the photoconversion of substrates in Ar-purged, air-equilibrated and O_2 saturated solutions).

Table 4. Conversion of substrate [a] and product distribution in the photolysis [b] of 4-allyl-tetrazolones **2a-c** in acetonitrile, cyclohexane and methanol.

Compound	Conditions	Substrate conversion (%)	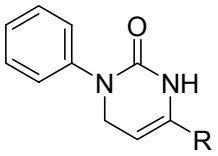	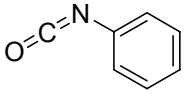	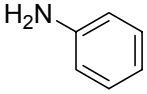	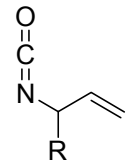 [c]
2a	CH_3CN (Ar-purged)	47	30	22	45	-
	CH_3CN (air-eq.)	84	26	20	52	-
	CH_3CN (O_2 sat.)	88	23	24	51	-
	Cyclohexane (Ar-purged)	34	29	31	37	-
	Cyclohexane (air-eq.)	66	31	29	37	-
	Cyclohexane (O_2 sat.)	71	31	26	40	-
	MeOH (Ar-purged)	48	96	-	-	-
	MeOH (air-eq.)	65	93	-	-	-
	MeOH (O_2 sat.)	78	95	-	-	-
2b	CH_3CN (Ar-purged)	48	21	32	41	-
	CH_3CN (air-eq.)	76	19	28	49	-
	CH_3CN (O_2 sat.)	79	20	28	45	-
	Cyclohexane (Ar-purged)	39	22	30	47	-
	Cyclohexane (air-eq.)	72	29	27	35	-
	Cyclohexane (O_2 sat.)	78	31	27	34	-
	MeOH (Ar-purged)	40	91	-	-	-
	MeOH (air-eq.)	73	92	-	-	-
	MeOH (O_2 sat.)	80	95	-	-	-
2c	CH_3CN (Ar-purged)	39	23	17	23	15
	CH_3CN (air-eq.)	70	17	24	21	14
	CH_3CN (O_2 sat.)	74	21	19	23	14
	Cyclohexane (Ar-purged)	36	31	14	24	19
	Cyclohexane (air-eq.)	56	21	17	30	23
	Cyclohexane (O_2 sat.)	69	25	19	24	20
	MeOH (Ar-purged)	39	92	-	-	-
	MeOH (air-eq.)	66	96	-	-	-
	MeOH (O_2 sat.)	70	95	-	-	-

[a] Relative yields in % determined by HPLC.
[b] Irradiation time: 20 min.; λ = 254 nm; concentration of substrate: 1.0×10^{-4} M.
[c] **2a** (R=H), **2b** (R=CH_3), **2c** (R=Ph).

One explanation for the increased photodegradation of **2a**–**c** in oxygen-saturated solutions could be the formation of an oxo-tetrazolone complex involving tetrazolone and O_2 molecules. This complex could reduce the influence of the solvent cage and increase photolysis quantum yields. In the oxygen/tetrazolone complex the relevant HOMO and LUMO orbitals might also have a smaller energy difference, favoring nitrogen elimination. However, our attempts to detect the formation of such ground-state complexes in the UV spectra were fruitless. Another, more plausible explanation for the sensitizing effect of the molecular oxygen could be acceleration of the T–S conversion in the triplet biradicals, opening the way to the formation of the product **6a**–**c** and consequently improving the photolysis quantum yields (see Scheme 1).

The quantum yield in function of oxygen concentration is given by expression (*2.5*), derived from the kinetic Scheme 1:

$$\phi = \phi_{pair} \frac{k_d + k_{ST} + k_q[O_2]}{k_d + k_{ST} + k_r + k_q[O_2]} \qquad (2.5)$$

where k_d is the first-order dissociation rate constant of the radical pair, k_r is its first-order recombination rate constant, k_{ST} is the intersystem conversion rate constant for the radical **2**–**2**, and k_q is its second-order reaction rate constant with dissolved oxygen. Figure 7 shows the product quantum yields in methanolic solutions for substances **2a**–**c** in function of the oxygen concentration.

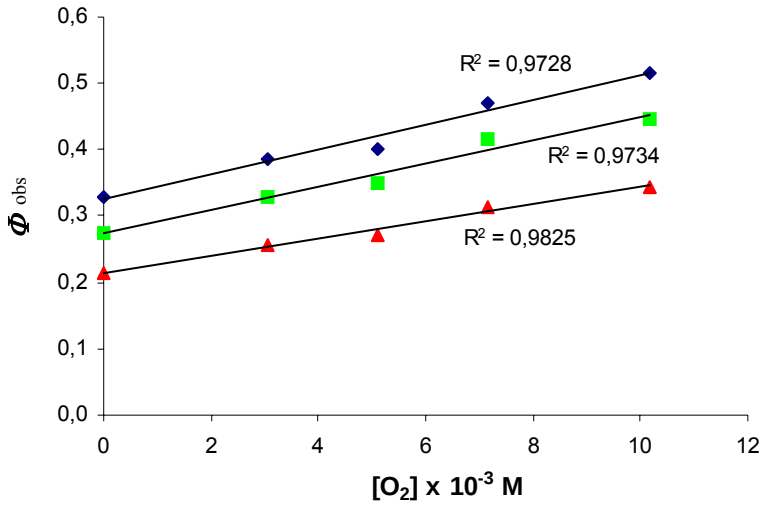

Figure 7. Plot of the product quantum yield as a function of oxygen concentration for 4-allyl-tetrazolones **2a** (◆), **2b** (■) and **2c** (▲) (methanolic solution).

We may use $k_q = 1 \times 10^{10}$ mol L^{-1} s^{-1}, equal to the diffusion-controlled reaction rate in methanol, thus obtaining an estimate $k_q[O_2] = 1 \times 10^8$ s^{-1} for the oxygen-induced S–T conversion rate at the highest oxygen concentrations used. The significant influence of the dissolved oxygen concentration on the product yields demonstrates that the rates of the other reactions in the Scheme 1 should be of comparable magnitude.

2.2.6. Conclusions

Photolysis of the 4-allyl-tetrazolones **2a**–**c** in methanol, 1-propanol and 1-hexanol solutions yields 3,4-dihydro-6-substituted-3-phenylpyrimidin-2(1*H*)-ones **5a**–**c** as sole products. These pyrimidinones are easily isolated from the alcoholic medium as stable compounds in excellent yields, providing an alternative and attractive synthetic methodology for this class of compounds. The observed photostability of pyrimidinones **5a**–**c** in alcohols is ascribed to a very efficient solvation, with formation of hydrogen bonds, leading to deactivation of the excited state by reversible proton transfer, facilitated by stable solvent cages that enclose the pyrimidinone molecules and prevent

their photodecomposition. The viscosity of the alcohols is directly related to the cage effects observed for 4-allyl-tetrazolones **2a**–**c**. Photoexcitation of 4-allyl-tetrazolones should involve formation of a caged triplet radical pair. This hypothesis is confirmed by the solvent viscosity effect on the photolysis quantum yields and by the fact that the presence of dissolved oxygen accelerated photodegradation. The relative yields of all the identified photoproducts remained similar to those obtained in oxygenated, air-equilibrated and Ar-purged systems. The reaction appears to occur via a triplet biradical intermediate **2**–**2** with the lifetime of ca. 10^{-8} s. Pyrimidinones **5a**–**c** form additional photoproducts in solvents other that alcohols, where the effect of the solvent hydrogen bonds upon the reactivity of their excited state is negligible.

2.3. Photochemistry of 5-Allyloxy-tetrazoles: Steady-state and Laser Flash Photolysis Study

Ongoing our promising studies on the photochemistry of allyl-tetrazolyl derivatives in solution, we present herein results on the reactivity of 5-allyloxy-tetrazoles (**1a-c**, Scheme 2) when exposed to the UV radiation in different solvents. Besides of our own interest in understanding the mechanism of photocleavage of these ethers, the possibility of isolation and characterization of reaction photoproducts may be particularly important for synthetic applications.

Scheme 2.

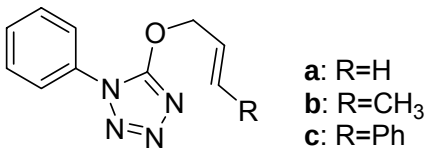

1

2.3.1. Steady-state Photolysis: Photoreactivity and Photoproduct Distribution

The 5-allyloxy-tetrazoles studied were synthesized from the corresponding allylic alcohols, initially converted into the alkoxides with sodium hydride, and then reacted with 5-chloro-1-phenyltetrazole, in a "one-pote" procedure.[9]

UV spectra of ethers **1a** and **1b** show absorption maxima around 230 nm, while the ether **1c** exhibits an intense absorption band at about 250 nm, due the bathochromic effect of the phenyl ring (Figure 8). The substrates dissolved in methanol, acetonitrile and cyclohexane were irradiated with a low-pressure mercury lamp (λ = 254 nm). The progress of the photoreactions was monitored by HPLC and GC-MS and the quantum yields for photocleavage were determined in each one of the tested solvents.

Figure 8 shows changes in the UV absorption spectra of compounds **1a**–**c** caused by the irradiation ($\lambda = 254$ nm) of their air-equilibrated methanolic solutions. For the compound **1a**, the absorption peak around 230 nm decreased with irradiation time, while a new absorption band grew at 238 nm. These spectral changes are very similar to those observed for derivative **1b**, indicating that the methyl group attached to the allylic chain exerts a negligible effect on the photoreactivity. Moreover, in the spectra of compounds **1a** and **1b** (Figure 8), the absorptivity at 254 nm registered for the new band belonging to the photoproducts is higher than that of the initial substrates at the same wavelength. This fact will significantly reduce the apparent photodecomposition rates of the two ethers, since the formed photoproducts absorb a larger part of the incident UV light. Interestingly, for ether **1c**, the reaction apparently seems to proceed faster than for compounds **1a** and **1b**, as seen from their absorption spectral changes, showing an isosbestic point at ≈ 275 nm. In Figure 8 (**1c**) we can observe that the absorptivity at 254 nm registered for the new bands belonging to the photoproducts is lower than that of the initial substrate at the same wavelength. For the derivative **1c**, the competition for the UV light between the photoproducts and the substrate is much less marked due to the absorption of the large part of the incident UV light by the substrate.

HPLC and GC-MS analysis of irradiated methanolic solutions of ethers **1a**–**c** led to the identification of one major photoproduct for each of the three derivatives. The primary photoproducts result from N_2 elimination from the tetrazolyl ring system through photo-induced cleavage of the two weakest N–N formally single bonds of the heterocycle, and were characterized as *N*-phenyl-1,3-oxazines **10a** (*m/z* = 174), **10b** (*m/z* = 188) and **10c** (*m/z* = 251) (see Figure 9).

Preparative-scale irradiations of the three tetrazolyl ethers in methanol were performed, aiming at the isolation of the primary photoproducts. These irradiations were carried out in cylindrical quartz cells with a 50 mm light path, using 50 mg of the starting material (see experimental section) and were controlled by TLC and HPLC.

Irradiation of the sample continued until the first detection of a secondary photoproduct. The remaining starting material was separated from the primary photoproduct by column chromatography on silica gel. Mass spectrometry (CI) and NMR analysis of the isolated primary extracts confirmed the structures of compounds **10a**–**c**.

Oxazines **10a**–**c** can adopt two tautomeric forms, depending on the position of the amino function on the molecule. The NH group can act as a bridge, connecting the oxazine and phenyl rings, or this group can be alternatively included in the oxazine ring. DFT calculations, performed at the B3LYP/6-31G(d,p) level of theory, carried out for the two tautomers of oxazines **10a** and **10b**, led to the identification, for both compounds, of two low-energy local minima when the NH group is connected to the two rings (structure **10(i)** in Figure 9), and of three low-energy local minima when the NH function is included in the oxazine ring (structure **10(ii)** in Figure 9). Calculations performed at the same level of theory for oxazine **10c** revealed nine low-energy local minima for the two tautomers of this compound: four minima with the NH group linking the phenyl and oxazine rings, and five minima with the NH included on the oxazine ring. All possible conformers and tautomers of oxazines **10a**–**c** have been theoretically investigated and the calculated Hessian matrices showed no imaginary frequencies, confirming that all the structures are true energy minima. Data for the most stable structure of oxazines is presented in Appendix A of this thesis (pages S4(A)-S5(A)).

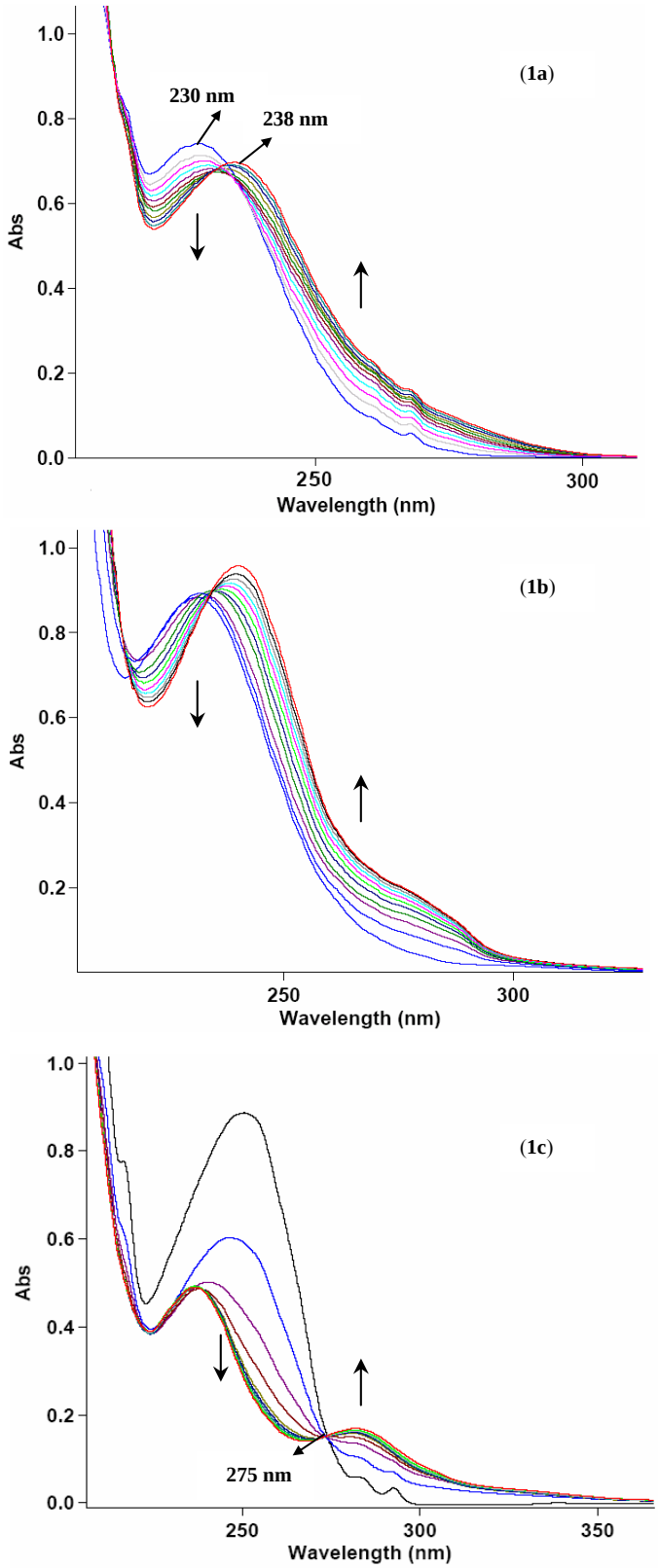

Figure 8. Changes in UV spectra of 5-allyloxy-tetrazoles **1a-c** in methanol (1×10^{-4} mol dm^{-3}) induced by UV irradiation (λ = 254 nm) at room temperature, with intervals of 30 s (**1a**, **1b**) and 15 s (**1c**). The vertical arrows indicate the evolution of absorbance with the irradiation time.

In order to estimate the conformational and tautomeric composition of compounds **10a**–**c** in solution, thermochemical calculations were carried out for all compounds at 25°C. Based on the calculated Gibbs free energies, the equilibrium Boltzmann populations were estimated for all tautomers/conformers and selected results are presented in Table 5.

Because of the significant energy differences between the tautomers **10(i)** and **10(ii)**, it can be expected that the population of oxazines at 25°C will be dominated by structures **10(i)**. Indeed, for all compounds **10a**–**c**, predicted populations of forms **10(i)** exceed 96% (see Table 5). The contribution of the minor tautomer **10(ii)** to the equilibrium mixture was predicted to be about 1.7% or more, for isolated molecules in vacuum. It is important to call attention to the fact that the total dipole moments of tautomers **10(ii)** are systematically higher than those of the tautomers **10(i)** (Table 5). It may be expected that, in the polar media, forms **10(ii)** will benefit from additional solvent stabilization, compared to forms **10(i)**, and the relative population of the minor conformer will increase. Based on this reasoning, we may conclude that both the tautomers **10(i)** and **10(ii)** will be relevant for further photolysis of oxazines **10a**–**c** in solution. Therefore, the secondary photoproducts of 5-allyloxy-tetrazoles **1a**–**c** may be formed via photodecomposition from forms **10(i)** and **10(ii)**, as presented in Figure 9.

Table 5. B3LYP/6-31G(d,p) calculated relative energies, populations and dipole moments for tautomers **(i)** and **(ii)** of oxazines **10a-c**.[a]

	Relative Energy (kJ mol^{-1})		Population (%)		Dipole Moment (Debye)	
Substrate	**(i)**	**(ii)**	**(i)**	**(ii)**	**(i)**	**(ii)**
10a	0	9.8	98.2	1.8	1.97	3.80
10b	0	7.6	96.0	4.0	1.63	4.21
10c	0	8.2	98.3	1.7	1.88	4.33

[a] Relative energies and dipole moments correspond to the most stable conformations of tautomers **(i)** and **(ii)**; populations correspond to the sum of populations of all conformers within a given tautomer, and were estimated based on the calculated relative Gibbs energies at 25°C.

We propose four different photochemical channels for the photodegradation of oxazines **10a**–**c** in methanol (routes ***A***-***D***, Figure 9).

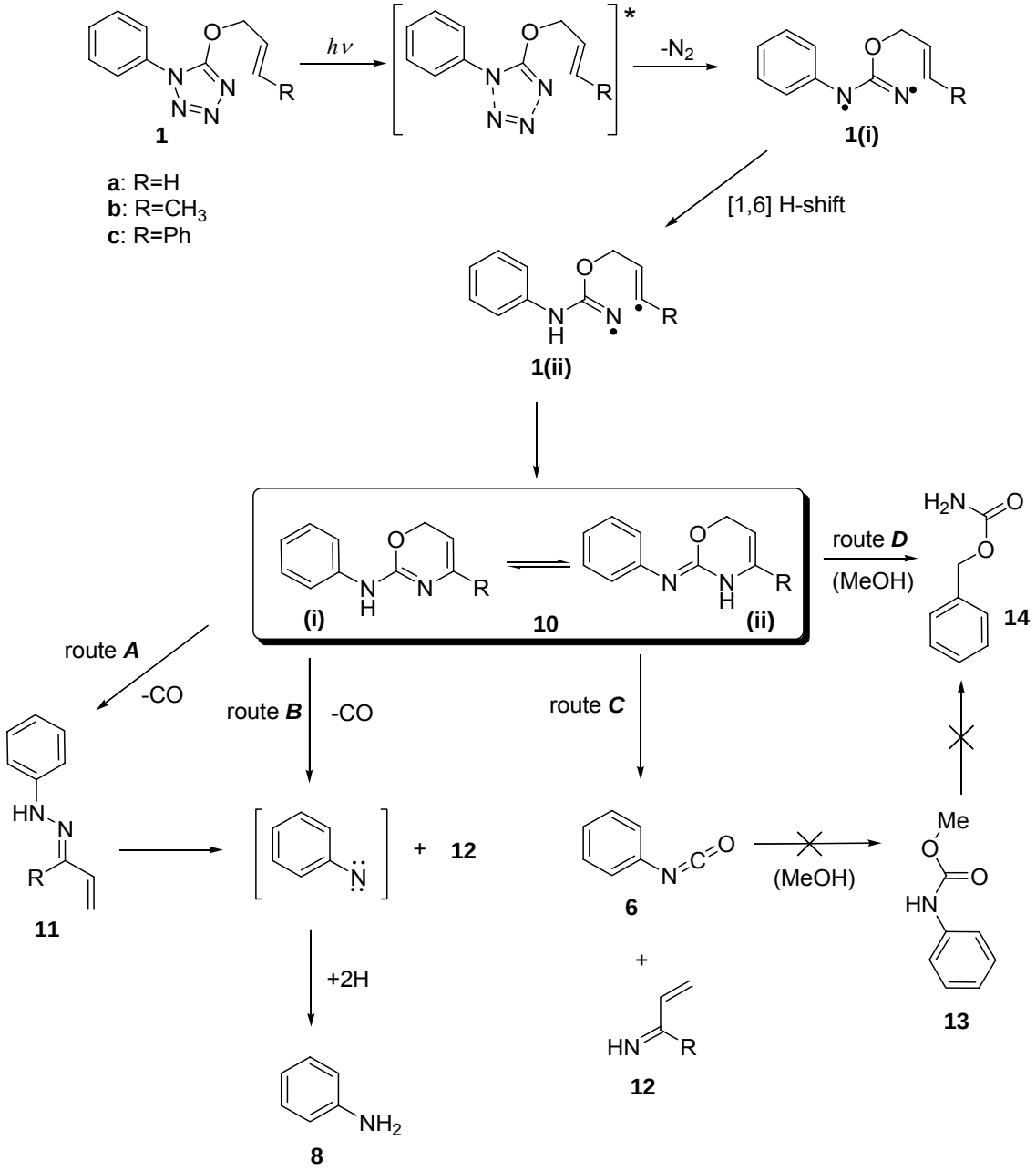

Figure 9. Proposed photodegradation pathways for 5-allyloxy-tetrazoles **1a-c**, in solution

In the first channel (route ***A***), photoproduct **11** (an allyl phenyl-hydrazine) is formed by extrusion of carbon monoxide from the oxazine ring. In the second photochemical channel (route ***B***), oxazine is directly converted, via a concerted mechanism, into aniline **8** and photoproduct **12**, also with CO extrusion.

The proposal of the independent photochemical channel (route ***A***) leading to the degradation of oxazine to form aniline and products **11** and **12**, is fully justified by the fact that product **11** and aniline start to be detected at the same reaction time. Upon continued exposure to UV radiation, even after complete decomposition of substrates **1a**–**c** into the primary photoproducts, we noted that the concentration of product **11** was decreasing, accompanied by a similar growth of aniline concentration. Hence, aniline and product **12** aren't exclusively a result of the oxazine photodecomposition *via* the concerted mechanism (route **B**), being also a product of photodecomposition of the photoproduct **11** (route ***A***). Probably, both routes ***A*** and ***B*** operate *via* the same transient species formed after absorption of a photon by the oxazine tautomers **10(i)** (Figure 9).

The production of aniline, straight from oxazine tautomers **10(i)** or by photodegradation of compound **11**, should involve in both cases the formation of the phenylnitrene intermediate [Ph–N:], which subsequently abstracts two hydrogen atoms from the environment, forming the product (see Figure 9). The possible source of the two hydrogen atoms, necessary to form aniline, will be discussed further in this work together with discussion of kinetics of the photoreactions.

The photoproducts **12a** (*m/*z = 55) and **12b** (*m/*z = 69), with the substituent groups R=H and R=CH_3, respectively, have never been detected chromatographically in the course of the irradiation experiments. This could be explained by their high volatility, fast photodecomposition into molecular products of lower weight, or very rapid elution in the chromatographic conditions used. On the other hand, the

photoproduct **12c** (R=Ph; *m/*z = 131) was clearly identified by GC-MS. The attribution of chemical structures for products **11** and **12** was based on their mass spectra, through the analysis of the fragmentation patterns exhibited. Aniline was easily identified by comparing the respective chromatogram with that of an authentic aniline sample.

A single photochemical channel is proposed for the formation of product **6** (phenylisocyanate). This species is formed *via* degradation of the minor oxazine tautomer **10(ii)** (route ***C***, Figure 9). As for aniline, phenylisocyanate was identified by using an authentic sample for comparison. Formation of phenylisocyanate in the photochemical channel ***C*** implies also formation of a by-product which is the same species as produced in routes ***A*** and ***B***, namely product **12**. Apparently, phenylisocyanate (obtained as a stable secondary photoproduct during the photolysis of 4-allyl-tetrazolones)[31] could undergo photocleavage to phenylnitrene [Ph–N:], with elimination of CO, which could then abstract hydrogen to form aniline. However, in view of the experimental observations, we consider that aniline and phenylisocyanate are produced via two independent photochemical channels of degradation of oxazine (routes ***A***/***B*** and ***C***, Figure 9). In the course of the irradiation experiments, the simultaneous formation of photoproducts **6** and **8** was detected, indicating that aniline does not derive from phenylisocyanate. This hypothesis was confirmed by HPLC analysis of irradiated solutions of phenylisocyanate in methanol, in conditions similar to those used for 5-allyloxy tetrazoles **1a**–**c**. Phenylisocyanate remained photostable upon prolonged irradiation at 254 nm, and no aniline formation was ever detected.

Another photoproduct was identified upon irradiation of ethers **1a**–**c** in methanolic solutions, namely benzyl carbamate (**10**, *m/z* = 151) (route ***D***, Figure 9). One possible explanation for appearance of compound **10** would be the rearrangement of methyl phenyl-carbamate (**13**, Figure 9), produced in the previous step of photolysis, via

the reaction of phenylisocyanate with a solvent molecule. To check this hypothesis, we have used an authentic sample of carbamate **13** and irradiated it in a methanolic solution under conditions similar to those used for the tetrazolyl ethers. However, chromatographic analysis demonstrated that benzyl carbamate is not a product of photodegradation of carbamate **13**. Therefore, at the present stage the reason of formation of benzyl carbamate upon the photolysis of tetrazolyl ethers **1a**–**c** remains unclear.

The kinetics of photodecomposition of 5-allyloxy-tetrazoles **1a**–**c** in methanolic solution is shown in Figure 10, along with kinetics of photoproducts formation. After 210 minutes of UV-irradiation, about 90% of the reagents **1a** and **1b** were consumed. The photodecomposition of ether **1c** occurs faster, with only 120 minutes required to achieve 90% transformation. After formation of the primary photoproducts **10a**–**c**, we found that, among the secondary photoproducts, the transformation of oxazines into phenylisocyanate (route ***C***, Figure 9) proceeds with the highest efficiency, as can be observed in Figure 10. This observation indicates that, in solution, the population of tautomer with the higher dipole moment, **10(ii)**, might be higher than that predicted for the gas phase on the basis of molecular orbital calculations. But more important is the fact that the population of **10(ii)** is constantly maintained as "small-but-present" due to dynamic equilibrium with **10(i)** in solution. Then, the photoreaction may be derived from the constantly repopulated **10(ii)**, if **10(i)** is not reactive (or not reactive enough) and serves as a source of **10(ii)**.

Figure 11 shows the changes in the UV absorption spectra of ethers **1a**–**c** upon UV-irradiation ($\lambda = 254$ nm) in air-equilibrated acetonitrile and cyclohexane solutions. The evolution of the UV absorption spectra reveals that the photoreactivity of **1a**–**c** should be very similar in acetonitrile and cyclohexane. The absorption band around 230

nm present in the spectra of compounds **1a** and **1b** decreased with irradiation time, while a new band grew at 238 nm.

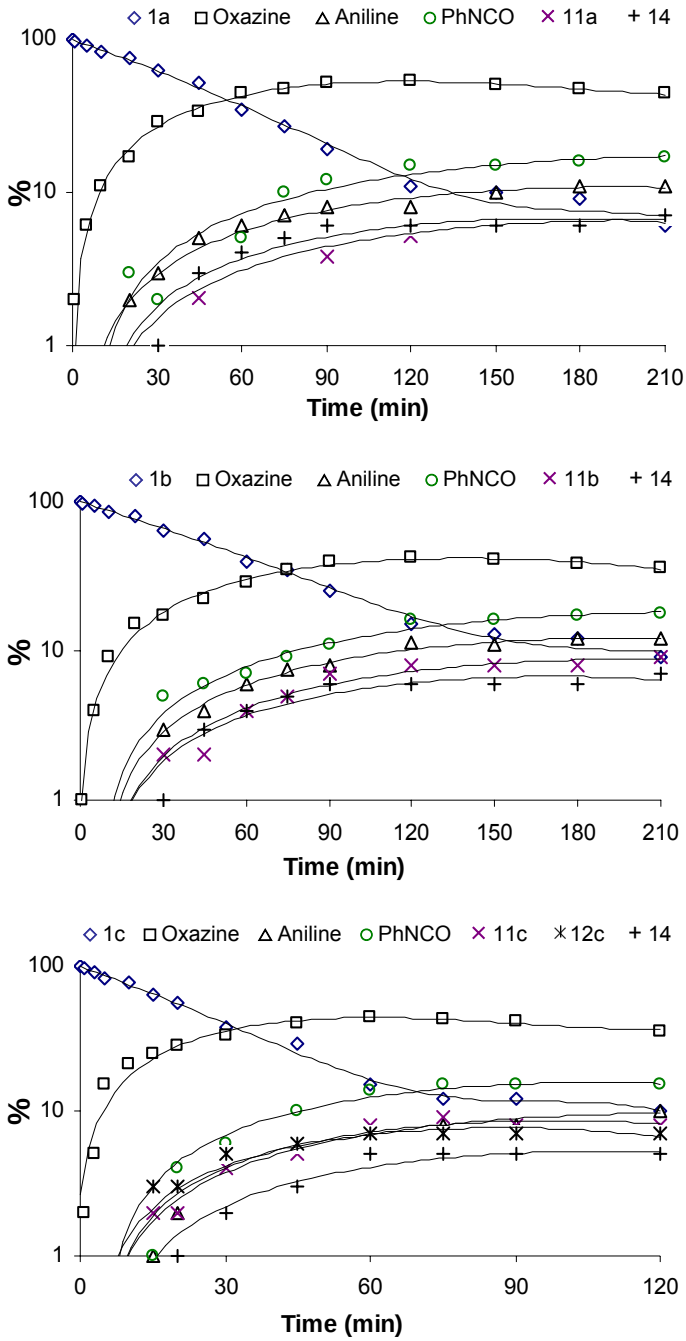

Figure 10. Time evolution of the amount of 5-allyloxy-tetrazoles **1a-c** and of photoproducts resulting from UV-irradiation (λ = 254 nm) in methanolic solution (1×10^{-4} mol dm^{-3}). The amount of reagent before irradiation was assumed to be 100%. The yields of different photoproducts were monitored by gaseous chromatography. Note that the ordinate scale is logarithmic.

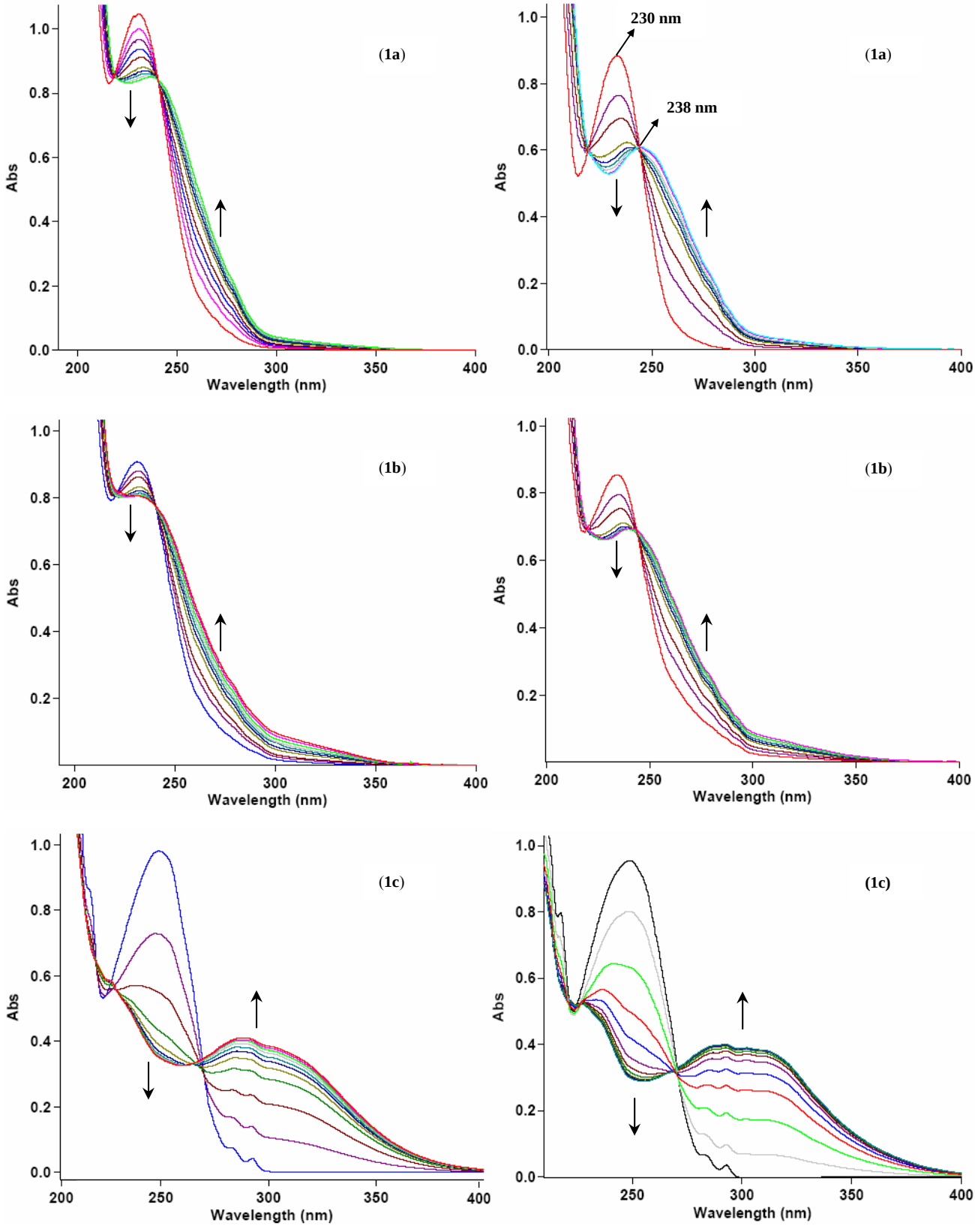

Figure 11. Changes in UV spectra of 5-allyloxy-tetrazoles **1a-c** in acetonitrile (*left*) and cyclohexane (*right*) (1×10^{-4} mol dm^{-3}) induced by UV irradiation ($\lambda = 254$ nm) at room temperature, with intervals of 30 s (**1a**, **1b**) and 15 s (**1c**). The vertical arrows indicate the evolution of absorbance with the irradiation time.

Figure 12 shows the kinetics for the photodecomposition of 5-allyloxy-tetrazoles (**3a–c**) in acetonitrile. As in methanol solutions, the photoreactivities of compounds **3a** and **3b** are very similar, whereas the photodecomposition of **3c** is faster. Both the reaction rates and the photoproduct distributions are very similar in the three solvents, with the extrusion of N_2 from the tetrazole ring remaining the sole primary process of photodegradation of tetrazoles **3a–c**, leading to the formation of oxazines **4a–c**.

Analysis of the kinetic results obtained for the photodegradation of ethers **3a–c** in the three tested solvents clearly shows that the effect of the nature of the solvent on the photoproduct distribution is very weak, *i.e.*, the relative percentage of photoproducts is maintained for all cases.

Analysis of the kinetics of photoreactions led us to propose a possible mechanism for aniline formation from phenyl-nitrene in photochannels **A**/**B**. All kinetics resemble each other very closely and occur in solvents that are very different from the viewpoint of proton-affinities: methanol, cyclohexane and acetonitrile. It is very unlikely that the two additional hydrogen atoms required for formation of aniline are provided by the solvent. Most probably, the compound itself undergoes an additional photochemical transformation resulting in abstraction of two H- atoms. This abstraction does not involve the three R-substituents (hydrogen, methyl, phenyl), since aniline formation is observed in all cases. We suggest that the two hydrogen atoms (the most labile H's) are abstracted from positions 3 and 6 of the oxazine ring of **10a–c** photoproducts in their **10(ii)** tautomeric form.

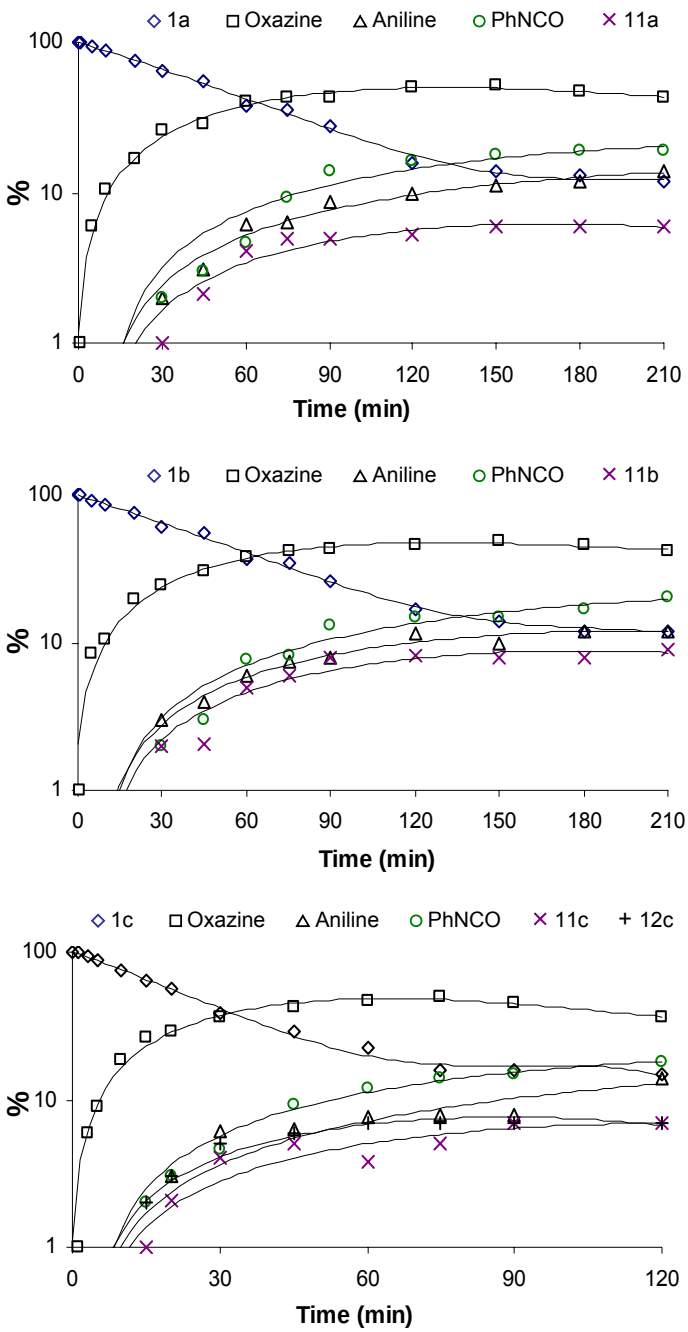

Figure 12. Time evolution of the amount of 5-allyloxy-tetrazoles **1a-c** and of photoproducts resulting from UV-irradiation (λ = 254 nm) in acetonitrile solution (1×10^{-4} mol dm^{-3}). The amount of reagent before irradiation was assumed to be 100%. The yields of different photoproducts were monitored by gaseous chromatography. Note that the ordinate scale is logarithmic.

The suggested mechanism for hydrogen abstraction is shown in Scheme 3. The optimized structures of derivatives **15a–c** are presented in Appendix A (pages S8(A)–S9(A)). An analogous photochemically induced hydrogen abstraction was reported for

1,4-cyclohexadiene in pentane solution[32] and the possibility of the occurrence of such a reaction was also shown theoretically.[33]

Scheme 3.

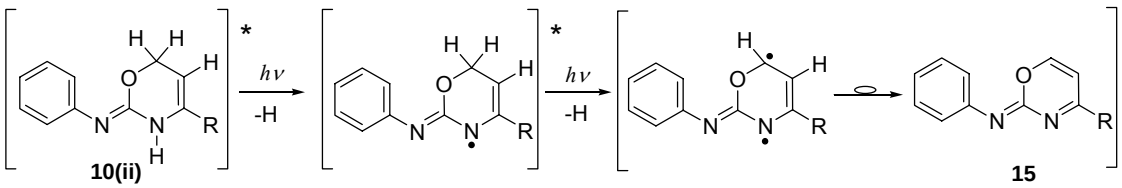

a: R=H, **b**: R=CH_3, **c**: R=Ph

Quantum yields for the photodecomposition of 5-allyloxy-tetrazoles **1a**–**c** were determined in the three solvents. Results are presented in Table 6 and show that the photoreactivity is very similar in acetonitrile and cyclohexane and is only slightly higher in methanol. Thus, the solvent effect on reactivity is indeed very weak. However, the enhancement of the photolysis quantum yield caused by the introduction of a phenyl on the allylic chain is much more pronounced.

Table 6. Quantum yields (Φ_{obs}) for the photodegradation of 5-allyloxy-tetrazoles **1a-c**, in the range of solvents used (λ = 254 nm, 25ºC).

Solvent (air-equilibrated)	**1a**, Φ_{obs}	**1b**, Φ_{obs}	**1c**, Φ_{obs}
CH_3CN	0.023	0.021	0.106
Cyclohexane	0.025	0.020	0.112
CH_3OH	0.037	0.035	0.144

2.3.2. Laser Flash Photolysis and Mechanistic Considerations

Laser flash photolysis of 5-allyloxy-tetrazoles **1a**–**c** in acetonitrile at 266 nm revealed formation of short-lived transient species, as detailed in Table 7. The transient decay for ether **1a** is apparently biexponential, with the contribution of the slower transient increasing at higher concentrations of the substrate. Therefore, we believe that the slower transient results from some kind of bi-photonic process, and will not discuss

it any further. The faster transient for the ether **1a** is spectrally similar to that of ether **1b**, presented in Figure 13 (top), with the lifetimes only slightly affected by the presence of dissolved oxygen. We identify these two transients as reactive radical species.

Table 7. Selected spectral and kinetic parameters for the transient species detected by laser flash-photolysis.[a]

	Transient 1		Transient 2	
Ether	**Lifetime, μs**	**λ_{max}, nm**	**Lifetime, μs**	**λ_{max}, nm**
1a (N_2, sat.)	2.2	350	13.8	310
1a (O_2, sat.)	1.3	330	10.0	290
1b (N_2, sat.)	0.8	300	--	--
1b (O_2, sat.)	0.7	320	--	--
1c (N_2, sat.)	2.3	290	--	--
1c (O_2, sat.)	0.5	290	--	--

[a] Results obtained in acetonitrile with excitation at 266 nm.

Laser flash photolysis of deaerated 0.1 mM solutions of tetrazole **1b** in acetonitrile solution yielded a wide transient absorption, with a maximum at 300 nm (see Figure 13). The lifetime of this species was around 800 ns under our experimental conditions.

The ether **1c** is once again a special case. The corresponding transient appears at shorter wavelengths, with the decay kinetics clearly accelerated by the dissolved oxygen (see Table 7). We identify this transient as a triplet excited state. Compared with ethers **1a**–**b**, the excited-state lifetime of the substrate **1c** is increased due to the presence of a larger electronic system, whereas the proton transfer reaction is further accelerated by the presence of the R=Ph substituent and does not limit the overall reaction kinetics any more. This justifies the identification of the transients observed for **1a**–**b** as radical species, and that for **1c** as the triplet excited state, further supported by the considerations that follow.

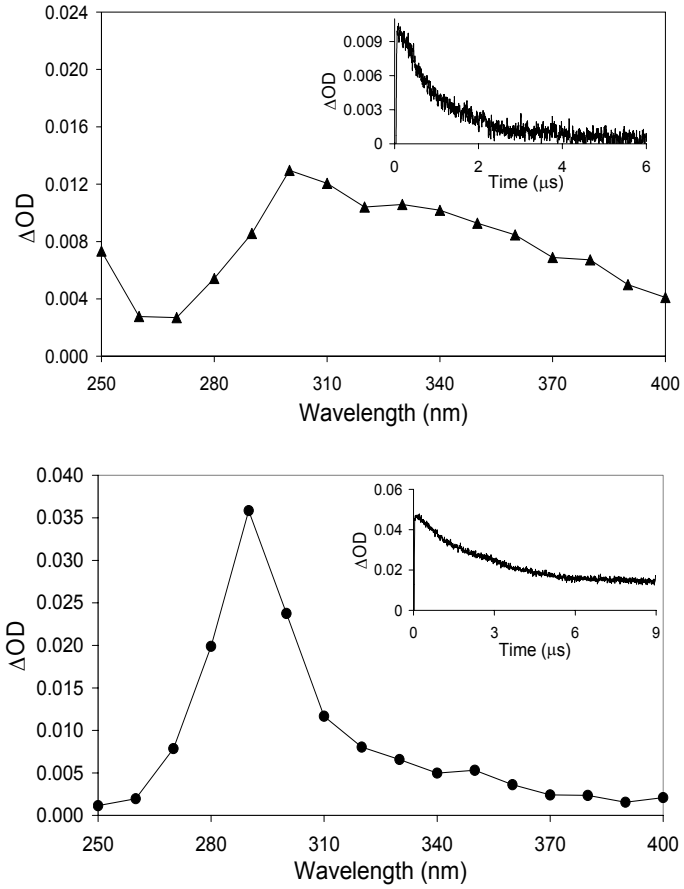

Figure 13. Absorption spectra calculated for the transient species formed upon laser excitation of **1b** (top) and **1c** (bottom) in acetonitrile (1×10^{-4} mol dm^{-3}), under nitrogen, immediately after the laser (266 nm) pulse. The inserts show decays, as monitored at 310 nm (**1b**, top) and 290 nm (**1c**, bottom).

Indeed, the photoinduced loss of nitrogen from tetrazoles **1a**–**c** may involve a cycloelimination leading to a diazirine that reacts further to give the observed oxazines **10a**–**c**, or may occur through a biradical intermediate that subsequently cyclises to give the same compounds **10a**–**c**. Usually, the transition state associated with a concerted mechanism (cleavage of two N–N formally single bonds and formation of one new N–N formally single bond and the transformation of N=N double bond into N≡N triple bond) has a higher polarity than the initial substrate. Considering the variation in polarity associated with the three solvents used in this work, it appears that the solvent polarity effects are weak or absent during tetrazole photolysis, contrasting with what could be expected for a concerted process occurring *via* a polar transition state.

It is well known that biradicals are among the most important intermediates in solution-phase organic photochemistry. However, and according to the literature, detection of these intermediates is not easy and could not be achieved in this work. In some related investigations, such species were detectable only in a limited number of cases.[34] On the other hand, based on the experimental results obtained, mainly on the lack of strong solvent effects, it is our conviction that a radicalar mechanism operates in this case.

Hence, we attribute the observed transients of 5-allyloxy-tetrazoles **1a** and **1b** to the triplet biradicals **1(i)** obtained through homolytic cleavage of two N–N single bonds, and the observed kinetics to the respective proton transfer reaction **1(i)** → **1(ii)** (see Figure 9). After conversion of triplet biradicals **1(ii)** into singlet biradicals *via* intersystem crossing, these intermediates decay to the ground state yielding the final products. Presumably, faster intersystem crossing occurs when the approach of both radical termini becomes easier. The transient for **1c** is strongly affected by dissolved oxygen, and is therefore identified as the triplet exited state of the substrate molecule. In this case the triplet excited state lives longer, whereas the proton transfer reaction **1(i)** → **1(ii)** operates faster, by influence of the phenyl substituent group, and therefore does not limit the overall reaction kinetics as happens for substrates **1a** and **1b**.

2.3.3. Conclusions

The results reported in this thesis answer several important mechanistic questions concerning the photochemistry of 5-allyloxy-tetrazoles **1a**–**c**. Photolysis of these compounds in the steady-state has been investigated in methanol, acetonitrile and cyclohexane solutions. Through this study we have shown that the exposure of tetrazoles **1a**–**c** to the UV light (λ = 254 nm) induces a primary photochemical process,

in which molecular nitrogen is eliminated, producing oxazines **10a**–**c**. In preparative-scale experiments, compounds **10a**–**c** were isolated from the reaction medium and fully characterized. DFT(B3LYP)/6-31G(d,p) calculations predict that, in the gaseous phase, oxazines **10a**–**c** should mostly exist in the tautomeric form where the NH group is the bridge connecting the oxazine and phenyl rings (the lowest-energy structures). The tautomers of **10a**–**c** with the NH function included in the oxazine ring are higher in energy, with the differences exceeding 7.5 kJ mol^{-1}, and have higher dipole moments. Accordingly, it is expected that, in the polar media, the higher-energy forms of oxazines will undergo additional stabilization with respect to the lowest-energy structures, and the relative population of the minor conformer will increase. In fact, secondary photoproduct analysis supports this interpretation. It is clear from the experiments that the presence of both oxazine tautomers is relevant in solution, increasing the number of secondary photodegradation channels in the three solvents. From these, phenyl vinyl-hydrazines **11a–c**, enamines **12a–c**, aniline and phenylisocyanate were obtained.

The pathway leading to production of phenylisocyanate predominates, this resulting from photocleavage of oxazine **10(ii)**. Kinetic results for the photodegradation of ethers **1a–c** in different solvents show that the effect of the nature of the solvent on the photoproduct distribution is very weak and the relative yields of photoproducts are maintained in all cases. However, there is a structural and a solvent effect on the photolysis quantum yields upon introduction of a phenyl on the allylic chain. Mechanistically, primary photoexcitation of 5-allyloxy-tetrazoles should involve formation of a triplet 1,3-biradical with a lifetime of *ca.* 10^{-6} s, which subsequently isomerizes to form a triplet 1,6-biradical. After intersystem crossing, the 1,6-biradical decays to the ground state to form the products.

2.4. Experimental Section

Equipment and experimental conditions. All chemicals were used as purchased from Aldrich. Solvents for extraction and chromatography were of technical grade. When required, the solvents used in reactions were freshly distilled from appropriate drying agents before use. Analytical TLC was performed with Merck silica gel 60 F_{254} plates. Melting points were recorded on a Stuart Scientific SMP3 melting point apparatus and are uncorrected. UV absorption spectra were recorded on a Varian CARY 50 Bio UV-Visible Spectrophotometer, using 1 × 1 cm quartz cells. Mass spectra were obtained on a VG 7070E mass spectrometer by electron ionization (EI, 70 eV) or chemical ionization (CI). ^{1}H NMR (400 MHz) spectra were obtained on a Bruker AM-400 spectrometer using TMS as the internal reference (δ = 0.0 ppm). Elemental analyses were performed on an EA1108-Elemental Analyzer (Carlo Erba Instruments). Infrared spectra were obtained as neat oils, or solids in NaCl on a Bruker FTIR-TENSOR 27 spectrometer. HPLC analyses were performed using an Agilent 1100 Series chromatograph with a 655A-22 UV detector and Shimadzu SPD-M6A Photodiode Array. A LiChroCART 125 column (RP-18, 5 μm, Merck) was used and the runs were performed using a mixture of water and acetonitrile (40:60) as the eluent. GC-MS analyses were carried out using a 6890-N Network GC System gas chromatograph with a 5973 *inert* Mass Selective Detector (E.I. 70 eV) of Agilent Technologies, using a DB-35MS capillary column with 30 m length and 0.25 mm I.D (J & W Scientific, Agilent). The initial temperature of 50 °C was maintained during 3 min and then a heating rate of 10 °C/min was applied, until a final temperature of 250 ºC was reached. Analyses were conducted on irradiated samples and on control solutions, kept in darkness. Controls showed no sign of degradation.

Optical bench irradiation system for 5-allyloxy-tetrazoles (1a-c). Steady-state photolysis experiments were carried out in acetonitrile, cyclohexane and methanol using, 1×1 cm fused-silica cells (Hellma) on a standard optical bench system. Photolyses were conducted with the cells at a distance of 10 to 40 cm from the Hg lamp. Generally, 10^{-4} M solutions of substrates were used when the analysis was carried out by UV-Visible absorption spectrophotometry. More concentrated solutions (10^{-2} M) were irradiated in the same conditions for product identification using GC-MS and HPLC. The 254 nm UV radiation was obtained using a 16W low-pressure mercury lamp (Applied Photophysics). A suitable interference filter was used to isolate the 254 nm line of the Hg lamp. Photolysis quantum yields were measured using the ferrioxalate actinometer.[35-37]

Optical bench irradiation system for 4-allyl-tetrazolones (2a-c). Photodegradation studies were conducted in a reactor previously used to investigate the photochemistry of pesticides,[38] employing a merry-go-round and an immersion-well photochemical reactor immersed in water for cooling. The water temperature was kept constant (25°C) using external circulation through a cooling bath. A 16 W low-pressure Hg lamp was used as source of the 254 nm UV radiation. Photolysis of tetrazolones **2a**–**c** was carried out in acetonitrile, cyclohexane, methanol, 1-propanol and 1-hexanol, using 1 cm quartz cells at 10 to 40 cm from the lamp. Generally, 10^{-4} M starting solutions were used when the analysis was carried out by HPLC. More concentrated 10^{-2} M solutions were used for product identification using GC-MS. Photolysis quantum yields were measured using the ferrioxalate actinometer.[35-37] A suitable interference filter was used to isolate the 254 nm line of the Hg lamp. Dissolved oxygen concentrations were varied by bubbling a controlled mixture of N_2 and O_2 through the solutions immediately before the photolysis, for 10 min.

Laser flash photolysis. Flash photolysis experiments were carried out on an Applied Photophysics LKS.60 laser-flash-photolysis spectrometer, with a Spectra-Physics Quanta-Ray GCR-130 Nd/YAG laser (fourth harmonic, 266 nm) for excitation and a Hewlett-Packard Infinium Oscilloscope for transient decay capture. Sample solutions were pumped through a quartz cell at a 0.8 mL min^{-1} flow rate (SSI chromatographic pump).

Computational methodology. The equilibrium geometries for compounds **2a–c**, **6**, **8**, **10a–c**, **11a–c**, **12a–c**, **13**, **14** and **15a–c** were fully optimized at the DFT level of theory with the standard 6-31G(d,p) basis set, using the Gaussian 98 or 03 programs.[39,40] DFT calculations were carried out with the B3LYP three-parameter density functional, which includes Becke's gradient exchange correction[41] and the Lee, Yang and Parr correlation functional.[42] No symmetry restrictions were imposed on the initial structures. Geometries, energies and Cartesian coordinates for the most stable conformers of molecules studied are included in Appendix A (pages S3(A)-S17(A)).

General procedure for the preparation of 5-allyloxy-tetrazoles 1a–c.

1-Phenyl-5-(prop-2-enyloxy) tetrazole (1a): prop-2-en-1-ol (allyl alcohol; 0.65 g; 11.1 mmol) in dry THF (10 mL) was added to a slurry of sodium hydride (55-60% in mineral oil; 0.72 g; 16.5 mmol) in dry THF (50 mL). The mixture was stirred at room temperature under an inert atmosphere until the effervescence had ceased (20 min.). 5-Chloro-1-phenyl-1*H*-tetrazole (2.0 g; 11.1 mmol) in dry THF (20 mL) was added and the mixture was stirred overnight at room temperature. The reaction was monitored by TLC using a mixture of toluene/acetone (5:1) as eluent. Ice-water (50 mL) was added and the organic product extracted with diethyl ether (3 × 50 mL). The combined organic extracts were dried (Na_2SO_4) and evaporated to dryness to give

1-phenyl-5-(prop-2-enyloxy) tetrazole as a light yellow oil (1.8 g; 80% yield). IR ν_{max}: 1592, 1556, 1500, 1456, 760 cm^{-1}; ^1H NMR ($CDCl_3$): δ 5.10 (2H, d, *J* 5.7 Hz), 5.30-5.60 (2H, m), 6.00-6.20 (1H, m), 7.40-7.60 (3H, m), 7.80 (2H, d, *J* 6.9 Hz) ppm; Anal. Calcd for $C_{10}H_{10}N_4O$: C, 59.4; H, 5.0; N, 27.7%; Found: C, 59.2; H, 5.1; N, 28.2%; MS (EI), *m*/*z* 202 $[M]^+$.

Similarly, other allyloxy-tetrazoles were prepared.

1-Phenyl-5-[(E)-but-2-enyloxy] tetrazole (1b): obtained from (*E*)-but-2-en-1-ol (crotyl alcohol; 1.0 g; 4.6 mmol) as light-yellow crystals (ethyl acetate, 67% yield), mp 36-37°C. IR ν_{max}: 1597, 1560, 1505, 1448, 761 cm^{-1}; ^1H NMR ($CDCl_3$): δ 1.75 (3H, d, *J* 8.7 Hz), 5.05 (2H, d, *J* 7.9 Hz), 5.72-5.90 (1H, m), 7.40-7.65 (3H, m), 7.75 (2H, d, *J* 8.3 Hz) ppm; Anal. Calcd for $C_{11}H_{12}N_4O$: C, 61.1; H, 5.6; N, 25.9%; Found: C, 61.1; H, 5.6; N, 26.0%; MS (EI), *m*/*z* 216 $[M]^+$.

1-Phenyl-5-[(E)-3-phenylprop-2-enyloxy] tetrazole (1c): obtained from (*E*)-3-phenylprop-2-en-1-ol (cinnamyl alcohol; 0.8 g; 2.9 mmol) as colourless needles (ethyl acetate, 72% yield), mp 67-68°C. IR ν_{max}: 1596, 1559, 1505, 1368, 757 cm^{-1}; ^1H NMR ($CDCl_3$): δ 5.25 (2H, d, *J* 7.0 Hz), 6.60 (1H, m), 6.85 (1H, d, *J* 15.6 Hz), 7.24-7.80 (10H, m) ppm; Anal. Calcd for $C_{16}H_{14}N_4O$: C, 69.9; H, 5.1; N, 20.2%; Found: C, 69.8; H, 5.0; N, 20.4%.; MS (EI), *m*/*z* 278 $[M]^+$.

Preparation of 4-allyl-tetrazolones 2a–c.

1-Phenyl-4-(prop-2-enyl) tetrazol-5-one (2a): 1-phenyl-5-(prop-2-enyloxy) tetrazole (1.0 g; 4.9 mmol) was heated neat in an oil bath at 150°C for 3 h to give the required 1-phenyl-4-(prop-2-enyl) tetrazole-5-one as the sole product (quantitative yield). IR ν_{max}: 1729, 1598, 1504, 1388, 757 cm^{-1}; ^1H NMR ($CDCl_3$): δ 4.65 (2H, d, *J* 5.7 Hz), 5.35-5.52 (2H, m), 5.92-6.10 (1H, m), 7.40-7.60 (3H, m), 8.05 (2H, d, *J* 6.86 Hz) ppm; Anal. Calcd for $C_{10}H_{10}N_4O$: C, 59.4; H, 5.0; N, 27.7%; Found: C, 59.8; H, 5.2; N, 28.1%; MS (EI), *m*/*z* 202 $[M]^+$.

4-(1-Methylprop-2-enyl)-tetrazol-5-one (2b): 1-phenyl-5-[(*E*)-but-2-enyloxy] tetrazole (1.0 g; 4.6 mmol) was heated neat in an oil bath at 150°C for 2 h to give 4-(1-methylprop-2-enyl)-tetrazole-5-one as the sole product (quantitative yield). IR ν_{max}: 1729, 1599, 1504, 1382, 757 cm^{-1}; ^1H NMR ($CDCl_3$): δ 1.65 (3H, d, *J* 5.7 Hz), 4.90-5.10 (1H, m), 5.22-5.40 (2H, m), 6.05-6.20 (1H, m), 7.30-7.55 (3H, m), 7.95 (2H, d, *J* 8.6 Hz) ppm; Anal. Calcd for $C_{11}H_{12}N_4O$: C, 61.1; H, 5.6; N, 25.9%; Found: C, 61.0; H, 5.6; N, 26.1%; MS (EI), *m*/*z* 216 $[M]^+$.

1-Phenyl-4-(1-phenylprop-2-enyl)-tetrazol-5-one (2c): 1-phenyl-5-[(*E*)-3-phenylprop-2-enyloxy] tetrazole (1.0 g; 3.6 mmol) was heated neat in an oil bath at 100°C for 2 h to give 1-phenyl-4-(1-phenylprop-2-enyl)-tetrazole-5-one as the sole product (quantitative yield). IR ν_{max}: 1729, 1598, 1504, 1382, 756 cm^{-1}; ^1H NMR ($CDCl_3$): δ 5.28-5.52 (2H, m), 6.00 (1H, d, *J* 5.7 Hz), 6.36-6.55 (1H, m), 7.30-7.52 (7H, m), 7.95 (2 H, d, *J* 8.6 Hz) ppm; Anal. Calcd for $C_{16}H_{14}N_4O$: C, 69.1; H, 5.1; N, 20.1%; Found: C, 68.8; H, 5.0; N, 20.4%; MS (EI), *m*/*z* 278 $[M]^+$.

General procedure for the preparation of pyrimidinones 5a–c (preparative scale irradiations).

3,4-Dihydro-3-phenylpyrimidin-2(1H)-one (5a): 1-phenyl-4-(prop-2-enyl) tetrazole-5-one **2a** (0.10 g; 0.49 mmol) in methanol (50 mL) was irradiated at 254 nm in a photochemical reactor using a 16 W low-pressure Hg lamp. Photolysis was conducted at a distance of 10 cm from the lamp. Gas formation in the solution was observed, corresponding to the photoeliminated molecular nitrogen. HPLC analysis indicated total absence of initial reagent after 3 h. The solvent was evaporated under reduced pressure at room temperature to give 3,4-dihydro-3-phenylpyrimidin-2(1H)-one **5a** as a yellow oil (0.078 g; 92% isolated yield). IR ν_{max}: 3212 (NH), 3054, 1693 (C=O), 1590, 1566, 1496, 1368, 1230, 1059, 756 cm^{-1}; ^1H NMR ($CDCl_3$): δ 4.65-4.68 (2H, d), 5.25-5.50 (1H, m), 7.12-7.20 (1H, m), 7.37-7.43 (2H, m), 7.50-7.57 (2H, t), 10.35 (1H, s) ppm; MS (EI), *m*/*z* 175 $[M+H]^+$; Acc. Mass (CI): Found = 175.12185, Calcd for $C_{10}H_{11}N_2O$: 175.12131.

Similarly, other pyrimidinones were prepared.

3,4-Dihydro-6-methyl-3-phenylpyrimidin-2(1H)-one (5b): from 4-(1-methylprop-2-enyl)-tetrazole-5-one **2b**, irradiated for 3.5 h, (97% isolated yield). IR ν_{max}: 3284 (NH), 3085, 1681 (C=O), 1598, 1548, 1484, 1446, 1378, 1230, 1068, 755 cm^{-1}; ^1H NMR ($CDCl_3$): δ 1.58-1.62 (2H, s), 3.75-3.78 (2H, d), 5.22-5.30 (1H, m), 6.15-6.25 (1H, m), 7.05-7.17 (2H, m), 7.25-7.42 (2H, m), 10.20 (1H, s) ppm; MS (EI), *m*/*z* 189 $[M+H]^+$; Acc. Mass (CI): Found = 189.10299, Calcd for $C_{11}H_{13}N_2O$: 189.10280.

3,4-Dihydro-3,6-diphenylpyrimidin-2(1H)-one (5c): from 1-phenyl-4-(1-phenylprop-2-enyl)-tetrazole-5-one **2c**, irradiated for 5 h, (90% isolated yield). IR ν_{max}: 3220 (NH), 3066, 1701 (C=O), 1581, 1543, 1422, 1345, 1226, 1066, 756 cm^{-1}; ^1H NMR ($CDCl_3$): δ 3.76-3.78 (2H, d), 5.42-5.48, (1H, m), 6.32-6.45 (1H, m), 6.70-6.75 (1H, m), 6.85-7.00 (2H, m), 7.10-7.35 (6H, m), 9.90 (1H, s) ppm; MS (EI), *m*/*z* 251 $[M+H]^+$; Acc. Mass (CI): Found = 251.11809, Calcd for $C_{16}H_{15}N_2O$: 251.11844.

General procedure for the preparation of compounds 10a–c (preparative scale irradiations). Irradiations at λ = 254 nm were carried out using a 10 mL cylindrical quartz cell with a 50 mm light path (Hellma). Solutions of ethers **1a**–**c** (50 mg in 10 mL of acetonitrile) were irradiated with continuous stirring, with the cell at a distance of 10 cm from the Hg lamp. The sample irradiation continued until detection of a secondary photoproduct, corresponding to the substrate conversion of about 30%, as monitored by HPLC analysis. At this point the solutions were removed and evaporated to concentrate the photoproducts. The photoproducts **10a**–**c** were isolated from the crude by column chromatography on silica gel, using a mixture of hexane and ethyl acetate as eluent. 1,3-Oxazines **10a**–**c** were obtained as light-yellow oils.

***N*-Phenyl-6*H*-1,3-oxazin-2-amine (10a).** Ether **1a** was irradiated during 10 h. The crude oil was chromatographed on silica gel (hexane/AcOEt 10:1), to give 15 mg (34%) of **10a** as a yellow oil. IR ν_{max}: 3270 (N–H), 1672, 1642, 1595, 1560, 1498, 1448, 1228, 1073, 1021, 992 and 759 cm^{-1}; ^1H NMR (400 MHz, $CDCl_3$): δ 4.22 (1H, s, N–H), 5.06-5.10 (2H, d, $-CH_2-$), 5.33-5.38 (1H, d, =CH–N), 6.05-6.08 (1H, m), 7.36-7.45 (1H, d), 7.46-7.52 (2H, t), 7.64-7.69 (2H, d) ppm; MS (EI), *m*/*z* 175 $[M+H]^+$; Acc. Mass (CI): Found = 175.1312, Calcd for $C_{10}H_{11}N_2O$: 175.1344.

4-Methyl-*N*-phenyl-6*H*-1,3-oxazin-2-amine (10b). Ether **1b** was irradiated during 10 h. The crude oil was chromatographed on silica gel (hexane/AcOEt 10:1), to give 13 mg (30%) of **10b** as a yellow oil. IR ν_{max}: 3264 (N–H), 2929, 1673, 1638, 1595, 1559, 1498, 1448, 1368, and 757 cm^{-1}; ^1H NMR (400 MHz, $CDCl_3$): δ 0.92 (3H, s, $–CH_3$), 4.20-4.24 (2H, t, $–CH_2–$), 5.02-5.08 (1H, t, =CH), 5.34 (1H, s, N–H), 7.45-7.54 (3H, m), 7.69-7.75 (2H, d) ppm; MS (EI), *m*/*z* 189 $[M+H]^+$; Acc. Mass (CI): Found = 189.2161, Calcd for $C_{11}H_{13}N_2O$: 189.2171.

***N*,4-Diphenyl-6*H*-1,3-oxazin-2-amine (10c).** Ether **1c** was irradiated during 6 h. The crude oil was chromatographed on silica gel (hexane/AcOEt 6:1), to give 15 mg (33%) of **10c** as a yellow oil. IR ν_{max}: 3255 (NH), 1678, 1597, 1543, 1498, 1444, 1314, 1250, 1223 and 752 cm^{-1}; ^1H NMR (400 MHz, $CDCl_3$): δ 4.79-4.81 (2H, d, $–CH_2–$), 5.42 (1H, s, N–H), 6.72-6.79 (1H, t, =CH), 7.28-7.33 (3H, m), 7.43-7.48 (4H, m), 7.55-7.60 (3H, m) ppm; MS (EI), *m*/*z* 251 $[M+H]^+$; Acc. Mass (CI): Found = 251.2312, Calcd for $C_{16}H_{15}N_2O$: 251.2312.

(See ^1H-NMR spectra of oxazines **10a-c** at pages S1(A)-S2(A), Appendix B).

2.5. References

1. Araújo, N.C.P.; Brigas, A.F.; Cristiano, M.L.S.; Frija, L.M.T.; Guimarães, E.M.O.; Loureiro, R.M.S. *J. Mol. Catal. A: Chem*. **2004**, *215*, 113.
2. Frija, L.M.T.; Cristiano, M.L.S.; Guimarães, E.M.O.; Martins, N.C.; Loureiro, R.M.S.; Bikley, J. *J. Mol. Catal. A: Chem*. **2005**, *242*, 241.
3. Araújo, N.C.P.; Barroca, P.M.M.; Brigas, A.F.; Cristiano, M.L.S.; Jonhstone, R.A.W.; Loureiro, R.M.S.; Pena, P.C.A. *J. Chem. Soc., Perkin 1* **2002**, *9*, 1213.
4. Kumar A.; Dittmer, D.C. *J. Org. Chem.* **1994**, *59*, 4760;
5. Adam, W.; Peters K.; Reuz, M. *Angew. Chem., Int. Ed. Engl.* **1994**, *33*, 1107;
6. Bergmeier, S.C.; Stanchina, D.M. *Tetrahedron Lett.* **1995**, *36*, 4533.
7. Bugalho, S.C.S.; Lapinskii, L.; Cristiano, M.L.S.; Frija, L.M.T.; Fausto, R. *Vibrational Spectroscopy* **2002**, *30*, 213.

8. Cristiano, M.L.S.; Johnstone, R.A.W.; Price, P.J. *J. Chem. Soc., Perkin 1* **1996**, 1453.
9. Cristiano, M.L.S.; Johnstone, R.A.W. *J. Chem. Soc., Perkin 2* **1997**, 489.
10. Cristiano, M.L.S.; Johnstone, R.A.W. *J. Chem. Res.* **1997**, 164.
11. Woodward, R.B.; Hoffmann, R. *"The Conservation of Orbital Symmetry" Verlag Chemie, GmbH, Weinheim*, 1970.
12. Ito, H.; Taguchi, T. *Chem. Soc. Rev.* **1999**, *28*, 43;
13. Ziegler, F.E. *Chem. Rev.* **1988**, *88*, 1423;
14. Dessolin, M.; Eisenstein, O.K.; Golfier, M.; Prange, T.; Sautet, P.G.N. *J. Chem. Soc., Chem. Commun. 2* **1992**, 132;
15. Boudjabi, S.; Dewynter, G.; Montero, J.L. *Synlett* **2000**, *5*, 716;
16. Metz, P.; Mues, C.; Schoop, A. *Tetrahedron* **1992**, *48*, 1071.
17. Frija, L.M.T.; Khmelinskii, I.V.; Cristiano, M.L.S. *Tetrahedron Lett.* **2005**, *46*, 6757.
18. Rovnyak, G.C.; Atwal, K.S.; Hedberg, A.; Kimball, S.D.; Moreland, S.; Gougoutas, J.Z.; O'Reilly, B.C.; Schwartz, J.; Malley, M.F. *J. Med. Chem.* **1992**, *35*, 3254.
19. Atwal, K.S. *et al. J. Med. Chem.* **1990**, *33*, 1510.
20. Matsuda, T.; Hirao, I. *Nippon Kagaku Zasshi* **1965**, *86*, 1195.
21. Sadanandam, Y.S.; Shetty, M.M.; Diwan, P.V. *Eur. J. Med. Chem.* **1992**, *27*, 87.
22. Kato, T. *Jpn. Kokai Tokkyo Koho JP* **1984**, *59*, 190, 974 [*Chem. Abstr.* **1985**, *102*, 132067].
23. Lagu, B. *et al. Bioorg. Med. Chem. Lett.* **2000**, *10*, 175.
24. Steele, T.G.; Coburn, C.A.; Patane, M.A.; Bock, M.G. *Tetrahedron Lett.* **1998**, *39*, 9315.
25. Kappe, C.O. *Tetrahedron* (review) **1993**, *49*, 6937.
26. Hu, E.H.; Sidler, D.R.; Dolling, U.-H. *J. Org. Chem.* **1998**, *63*, 3454.
27. Solntsev, K.M., Huppert, D., Agmon, N., Tolbert, L.M. *J. Phys. Chem. A,* **2000**, *104,* 4658.
28. Lide, D.R. Editor-on-chief, *CRC-Handbook of Chemistry and Physics,* on CD-ROM, CRC Press, *version* 2002.
29. Braden, D.A.; Parrack, E.E.; Tyler, D.R. *Coordination Chemistry Reviews* **2001**, *211*, 279.
30. Turro, N.J. *Photoaddition and photosubstitution reactions. In: Modern Molecular Photochemistry*, The Benjamin / Cummings Publishing Co., Inc., California, 1978, pp. 362-413.
31. Frija, L.M.T.; Khmelinskii, I.V.; Cristiano, M.L.S. *J. Org. Chem.* **2006**, *71*, 3583.
32. Zimbros, S.; Haas, Y. *Phys. Chem. Chem. Phys*. **2002**, *4*, 34.
33. De Feyter, S. ; Diau, E.W.-G.; Zewail, A.H. *Phys. Chem. Chem. Phys.*, 2000, **2**, 877.
34. Dunkin, I.R; Shields, C.J.; Quast, H. *Tetrahedron*, 1989, **45**, 259.
35. Parker, C.A. *Proc. R. Soc. London, Ser. A.* **1953**, *220*, 104.
36. Hatchard, C.G.; Parker, C.A. *Proc. R. Soc. London, Ser. A.* **1956**, *235*, 518.
37. Calvert, J.G.; Pitts, J.N.Jr. *Photochemistry*, John Wiley and Sons, New York, 1967, pp. 769-804.
38. Da Silva, J.P.; Da Silva, A.M.; Khmelinskii, I.V.; Martinho, J.M.G.; Vieira Ferreira, L.F. *J. Photochem. Photobiol. A: Chem.* **2001**, *142*, 31.

39. Frisch, M.; Trucks, G.; Schlegel, H.; Scuseria, G.; Robb, M.; Cheeseman, J.; Zakrzewski, V.; Montgomery, J.; Stratmann, R.; Burant, K.; Dapprich, S.; Millam, J.; Daniels, A.; Kudin, K.; Strain, M.; Farkas, O.; Tomasi, J.; Barone, V.; Cossi, M.; Cammi, R.; Mennucci, B.; Pomelli, C.; Adamo, C.; Clifford, S.; Ochterski, J.; Petersson, G.; Ayala, P.; Cui, Q.; Morokuma, K.; Malick, D.; Rabuck, A.; Raghavachari, K.; Foresman, J.; Cioslowski, J.; Ortiz, J.; Baboul, A.; Stefanov, B.; Liu, G.; Liashenko, A.; Piskorz, P.; Komaromi, I.; Gomperts, R.; Martin, R.; Fox, D.; Keith, T.; Al-Laham, M.; Peng, C.; Nanayakkara, A.; Challacombe, M.; Gill, P.; Johnson, B.; Chen, W.; Wong, M.; Andres, J.; Gonzalez, C.; Head-Gordon, M.; Replogle, S.; Pople, J., Gaussian 98, Revision A.9, Gaussian Inc. Pittsburgh, PA 1998.
40. Frisch, M.J.; Trucks, G.W.; Schlegel, H.B.; Scuseria, G.E.; Robb, M.A.; Cheeseman, J.R.; Montgomery, J.A.; Vreven, T.; Kudin, K.N.; Burant, J.C.; Millam, J.M.; Iyengar, S.S.; Tomasi, J.; Barone, V.; Mennucci, B.; Cossi, M.; Scalmani, G.; Rega, N.; Petersson, G.A.; Nakatsuji, H.; Hada, M.; Ehara, M.; Toyota, K.; Fukuda, R.; Hasegawa, J.; Ishida, M.; Nakajima, T.; Honda, Y.; Kitao, O.; Nakai, H.; Klene, M.; Li, X.; Knox, J.E.; Hratchian, H.P.; Cross, J.B.; Bakken, V.; Adamo, C.; Jaramillo, J.; Gomperts, R.; Stratmann, R.E.; Yazyev, O.; Austin, A.J.; Cammi, R.; Pomelli, C.; Ochterski, J.W.; Ayala, P.Y.; Morokuma, K.; Voth, G.A.; Salvador, P.; Dannenberg, J.J.; Zakrzewski, V.G.; Dapprich, S.; Daniels, A.D.; Strain, M.C.; Farkas, O.; Malick, D.K.; Rabuck, A.D.; Raghavachari, K.; Foresman, J.B.; Ortiz, J.V.; Cui, Q.; Baboul, A.G.; Clifford, S.; Cioslowski, J.; Stefanov, B.B.; Liu, G.; Liashenko, A.; Piskorz, P.; Komaromi, I.; Martin, R.L.; Fox, D.J.; Keith, T.; Al-Laham, M.A.; Peng, C.Y.; Nanayakkara, A.; Challacombe, M.; Gill, P.M.W.; Johnson, B.; Chen, W.; Wong, M.W.; Gonzalez, C.; Pople, J. A. Gaussian 03, Revision C.02 ed.; Gaussian, Inc.: Wallingford CT, 2004.
41. Becke, A.D. *Phys.Rev. B: Condens. Matter* **1988**, *38*, 3098.
42. Lee C.; Yang, W.; Parr, R.G. *Phys.Rev. B: Condens. Matter* **1988**, *37*, 785.